Hippocampal-parietal cortex causal information flow in human episodic memory: replication across three experiments

Anup Das[1] and Vinod Menon[1,2,3]

Department of Psychiatry & Behavioral Sciences[1]
Department of Neurology & Neurological Sciences[2]
Wu Tsai Neurosciences Institute[3]
Stanford University School of Medicine
Stanford, CA 94305

Corresponding author email address: a1das@stanford.edu, menon@stanford.edu

Conflict of interest statement: The authors declare no competing financial interests.

Acknowledgements

This research was supported by NIH grants NS086085 and EB022907.

Abstract

While extensive research has focused on hippocampus-prefrontal circuits in episodic memory and spatial navigation, the role of hippocampus-parietal cortex circuits remains understudied. We employed intracranial EEG to investigate these circuits across three different memory experiments, revealing a consistent, asymmetric pattern of higher causal information flow from the hippocampus to both lateral and medial posterior parietal cortex (PPC). This directional information flow was observed during both memory encoding and recall and across verbal and spatial episodic memory domains. Importantly, this directed information flow was not contingent upon activation or suppression states in the hippocampus or PPC. Frequency-specific directional interactions were also identified, with greater hippocampal-to-PPC flow in the delta-theta band and the reverse in the beta band. The robustness of these results was demonstrated through Bayesian replication analysis. Our findings shed new light on the frequency-dependent signaling within hippocampus-parietal circuits, broadening our understanding of their critical roles in human episodic memory.

Introduction

Episodic memory, the recollection of specific events and experiences, is central to human cognition (Tulving, 2002). The formation of episodic memories is thought to be supported by distributed brain circuits that integrate neural and cognitive processes involved in encoding and recall of specific events and experiences (Moscovitch, Cabeza, Winocur, & Nadel, 2016). While the hippocampus has been long recognized as a key brain structure for memory formation (Burgess, Maguire, & O'Keefe, 2002), a growing body of research is uncovering a key role for the parietal cortex in memory recall and recollection, expanding our understanding of the neurocognitive processes involved in episodic memory (Cabeza, Ciaramelli, Olson, & Moscovitch, 2008; Curtis, 2006; Husain & Nachev, 2007; Rolls, 2018, 2019; Vogt & Pandya, 1987; Wagner, Shannon, Kahn, & Buckner, 2005; Whitlock, Sutherland, Witter, Moser, & Moser, 2008). However, the electrophysiological correlates of their dynamic circuit interactions and specific spectral-temporal characteristics of how hippocampus-parietal circuits operate during human memory formation remain poorly understood.

Although previous studies predominantly emphasized the significance of hippocampus-prefrontal circuits in episodic memory (Dickerson & Eichenbaum, 2010; Eichenbaum, 2017; Moscovitch et al., 2016), there is growing evidence that hippocampus-parietal circuits also play a pivotal role in episodic memory (Simons, Ritchey, & Fernyhough, 2022). Despite its importance, this circuitry has received comparatively less attention in the scientific literature, leaving a significant gap in our understanding of its functional relevance in memory encoding and retrieval. Our study aims to address this gap by investigating the electrophysiological dynamics between the hippocampus and the parietal cortex, thereby contributing to a more comprehensive understanding of the neural mechanisms underlying episodic memory in the human brain.

Here, we leverage a large sample of intracranial EEG (iEEG) recordings, from 98 participants and three separate memory experiments, and investigate the temporal dynamics of signaling between the hippocampus and multiple distinct anatomical subdivisions of the parietal cortex. Spanning memory encoding and recall across both verbal and spatial domains, our study aims to unveil the causal dynamics of hippocampal-parietal interactions, enriching our understanding of episodic memory's neural architecture and bridging important gaps in our current knowledge.

Extensive research in rodents and non-human primates has laid the groundwork for understanding the role of the hippocampus and parietal cortex in spatial memory. Single-neuron studies in these models have identified the posterior parietal cortex (PPC) as a key neural substrate for spatial memory tasks (Andersen, Essick, & Siegel, 1985; Chen, Lin, Green, Barnes, & McNaughton, 1994; Crowe, Chafee, Averbeck, & Georgopoulos, 2004; McNaughton et al., 1994; Nitz, 2006). Further, lesion studies have not only reinforced the importance of the parietal cortex in memory tasks (Barrow & Latto, 1996; Goodrich-Hunsaker, Hunsaker, & Kesner, 2005; Rogers & Kesner, 2006), but have also highlighted the crucial connectivity between the hippocampus and PPC for successful memory retrieval (Rogers & Kesner, 2007). These interactions are likely subserved by direct anatomical pathways, as anterograde and retrograde tracing studies in non-human primates have uncovered bidirectional projections between the hippocampus and PPC (Clower, West, Lynch, & Strick, 2001; Insausti & Muñoz, 2001; Rockland & Van Hoesen, 1999), reinforcing their interconnected relationship. However, a

translational gap exists, as the electrophysiological correlates of hippocampus-parietal circuit function have not been fully explored in human studies, a limitation our research aims to address.

In human studies, functional magnetic resonance imaging (fMRI) has consistently shown that both the hippocampus and the parietal cortex are engaged during memory encoding and recall, as evidenced by a multitude of studies (Auger & Maguire, 2013; Benoit & Schacter, 2015; Brodt et al., 2018; Brodt et al., 2016; Buckner et al., 1998; Ciaramelli, Burianová, Vallesi, Cabeza, & Moscovitch, 2020; Gurd et al., 2002; Jonker, Dimsdale-Zucker, Ritchey, Clarke, & Ranganath, 2018; Konishi, Wheeler, Donaldson, & Buckner, 2000; Korkki, Richter, & Simons, 2021; Leech & Sharp, 2014; Miyamoto et al., 2013; Spreng, Stevens, Chamberlain, Gilmore, & Schacter, 2010; Summerfield, Hassabis, & Maguire, 2010; Vincent et al., 2006). Event-related potentials using scalp EEG recordings have illuminated the temporal aspects of brain activity, highlighting the role of the PPC in successful memory retrieval (Paller, Kutas, & McIsaac, 1995; Paller, McCarthy, Roessler, Allison, & Wood, 1992; Paller, McCarthy, & Wood, 1988; Rugg et al., 1998; Wilding & Rugg, 1996). Further substantiating this line of inquiry, magnetoencephalography studies have suggested dissociable roles for delta, theta, and beta rhythms within PPC during the recall phase of episodic memory (Osipova et al., 2006; Seibert, Hagler, & Brewer, 2011).

Building on this, human iEEG depth recordings have confirmed the parietal cortex's role in episodic memory encoding and recall, as reflected in enhanced high-gamma frequency band activity (Gonzalez et al., 2015; Rubinstein et al., 2021; Tan, Rugg, & Lega, 2020). These studies also reveal a theta frequency band correlation between hippocampus and PPC in tasks involving virtual spatial navigation (Ekstrom et al., 2005). Complementing these findings, transcranial stimulation studies have illustrated enhanced information flow between the parietal cortex and the hippocampus, resulting in improved memory performance (Crossman, Bartl, Soerum, & Sandrini, 2019; J. X. Wang et al., 2014). However, the precise nature of bidirectional interactions between the hippocampus and PPC, along with their frequency specificity, remains largely unexplored. Critically, the question of whether hippocampus-parietal circuity operate similarly in the verbal and spatial domains has not been addressed. This leaves a critical gap in our understanding of how the hippocampus interacts with the various anatomical subdivisions of the PPC to support human episodic memory across different cognitive contexts.

The human parietal cortex is marked by a unique heterogeneity, featuring subdivisions that have undergone significant evolutionary expansion in comparison to rodents and non-human primates (Goldring & Krubitzer, 2020). Both the lateral and medial PPC have undergone significant expansion. On the lateral surface, the dorsal PPC primarily comprised of the supramarginal gyrus and intraparietal sulcus are engaged in a wide range of tasks requiring spatial attention. In contrast, the ventral PPC encompassing the angular gyrus is crucial for the retrieval of vivid details and schema-based information (Buckner, Andrews-Hanna, & Schacter, 2008; Corbetta, 1998; Rugg & Vilberg, 2013). Notably, neither rodent nor non-human primate brains include an angular gyrus subdivision leaving unclear the dynamic interactive roles these parietal subdivisions play in episodic memory. Furthermore, the angular gyrus, together with the posterior cingulate cortex (PCC)/precuneus in the medial PPC, serve as core nodes of the default mode network. This network is typically deactivated during tasks that demand external attention (Bressler & Menon, 2010; Garrison et al., 2013; Greicius, Krasnow, Reiss, & Menon, 2003;

Raichle et al., 2001; Zhang & Li, 2012), further suggesting a demarcation of their roles in episodic memory. The anatomical and functional complexity of the human PPC necessitates a more precise examination of its role in hippocampal-parietal circuitry for memory formation (Sestieri, Shulman, & Corbetta, 2017). Our study aims to fill this gap by investigating the electrophysiological dynamics between the hippocampus and key subdivisions of the PPC, both in its lateral and medial aspects. This focus allows for a more comprehensive understanding of hippocampal-parietal circuits, addressing a critical, yet overlooked area in the existing literature.

We leveraged iEEG data from the UPENN-RAM consortium (Solomon et al., 2019) to address critical gaps in our understanding of the electrophysiological mechanisms underpinning hippocampal-parietal cortex interactions in memory formation. This dataset includes depth recordings from an extensive cohort of individuals, allowing us to rigorously investigate the directionality and frequency specificity of information flow between the hippocampus and multiple subdivisions of the lateral and medial parietal cortex. We employed three distinct episodic memory experiments: (i) a verbal free recall (VFR) task, in which participants were presented with a sequence of words for subsequent verbal recall, (ii) a categorized verbal free recall (CATVFR) task, which similarly involved encoding and recalling a sequence of words, but with the added demands of categorical organization, and (iii) a water maze spatial memory (WMSM) task, wherein participants were required to memorize the spatial location of the objects for subsequent recall. These comprehensive datasets afforded a unique opportunity to probe hippocampal-parietal cortex interactions across memory encoding and recall phases and multiple cognitive domains.

The first objective of our study was to delineate the directed, causal information flow between the hippocampus and multiple subdivisions of the lateral and medial PPC during verbal and spatial memory tasks. To accomplish this, we employed phase transfer entropy (PTE) (Hillebrand et al., 2016; Lobier, Siebenhühner, Palva, & Matias, 2014; M. Y. Wang et al., 2017). PTE provides a robust quantitative measure for characterizing directional information flow, capturing linear as well as nonlinear dynamics in iEEG data (Hillebrand et al., 2016; Lobier et al., 2014; Menon et al., 1996).

We examined three main hypotheses to guide our analysis. First, based on the 'top-down attention' hypothesis related to the dorsal PPC in memory encoding (Cabeza, 2008; Cabeza, Ciaramelli, & Moscovitch, 2012; Cabeza et al., 2011; Ciaramelli, Grady, & Moscovitch, 2008; Daselaar et al., 2009; Hutchinson, Uncapher, & Wagner, 2009; Uncapher & Wagner, 2009), we predicted that causal influences from the dorsal PPC to the hippocampus would be more pronounced compared to the reverse influence during the encoding phase. Second, based on the bottom-up attention hypothesis of the ventral PPC in memory recall (Cabeza et al., 2008), we hypothesized that causal influences from hippocampus to ventral PPC would be stronger compared to the reverse direction. Third, we extended our hypotheses to the interactions between the hippocampus and the PCC/precuneus. We posited that the hippocampus would exert stronger influence on the PCC/precuneus during memory recall, mirroring its dynamics with the ventral PPC. This hypothesis is grounded in the fact that both the PCC/precuneus and the ventral PPC are integral nodes of the DMN, a brain network known to be involved in episodic memory recall and internally-driven cognition (Menon, 2023).

Our second objective was to investigate the frequency-specificity of causal interactions between the hippocampus and parietal cortex. Prior research across various species, including rodents, non-human primates, and humans, have emphasized the prominent functional roles of distinct frequency bands. Specifically, the delta-theta rhythm (0.5-8 Hz) has been identified as crucial in hippocampal functions (Ekstrom & Watrous, 2014; Neuner et al., 2014; Watrous, Tandon, Conner, Pieters, & Ekstrom, 2013), while beta-band rhythms (12-30 Hz) have been highlighted in the parietal cortex (Brovelli et al., 2004; Engel & Fries, 2010; Spitzer & Haegens, 2017; Stanley, Roy, Aoi, Kopell, & Miller, 2018). It has been suggested that delta-theta oscillations may facilitate synchronization between hippocampus and parietal cortex (Ekstrom & Watrous, 2014), while beta band oscillations may serve to coordinate neuronal activity with other cortical and subcortical structures (Engel & Fries, 2010; Negrón-Oyarzo et al., 2018; Spitzer & Haegens, 2017). However, the frequency-specificity of directed causal interactions between the hippocampus and parietal cortex during verbal and spatial memory remains an open question. We hypothesized that the hippocampus would exert a stronger "feedforward" causal influence on both the lateral PPC and PCC/precuneus in the delta-theta band. Conversely, we posited that the PPC and PCC/precuneus would have a stronger "top-down" causal influence on the hippocampus in the beta band.

Our third objective was to probe regional profiles of neural response in the hippocampus and the three specific lateral and medial PPC subdivisions. High-gamma band activity reflects localized, task-related neural processing, and is associated with synchronized activity of local neural populations (Canolty & Knight, 2010). Moreover, increases in high-gamma power correlate with elevated neuronal spiking and synaptic activity, making it a robust marker for task-specific computations within local neuronal circuits (Ray, Crone, Niebur, Franaszczuk, & Hsiao, 2008). We determined whether high-gamma band power in these parietal subdivisions exhibits context-dependent variations across two critical phases of memory formation—encoding and recall. Given that memory encoding is largely influenced by external stimuli, we anticipated distinct neural response patterns in this phase compared to memory recall, which is mainly internally driven (Andrews-Hanna, 2012; Buckner et al., 2008). Specifically, we hypothesized that high-gamma power in the ventral PPC and the PCC/precuneus, regions associated with the DMN, would be reduced during the encoding phase, reflecting the externally-driven nature of the task. Conversely, we expected an increase in high-gamma power during the recall phase, which requires more internally-oriented cognition. Furthermore, we expected the dorsal PPC, which is more engaged in tasks requiring adaptive external response, to show differential modulations in high-gamma power during both encoding and recall phases. These analyses aimed to provide complementary information on the differential roles played by these brain regions in the orchestration of episodic memory formation.

Our final objective was to assess the robustness and replicability of our findings across three distinct episodic memory experiments, encompassing the verbal and spatial domains. Replicability poses a significant challenge in the field of neuroscience, and this issue is particularly acute in invasive iEEG studies, where difficulty of acquiring data, small sample sizes, and lack of data sharing often hinder the generalizability of findings. To address this 'reproducibility crisis', we employed Bayesian analysis which provides a robust quantitative approach that allows for the explicit quantification of evidence for or against a given hypothesis (Ly, Etz, Marsman, & Wagenmakers, 2019; Verhagen & Wagenmakers, 2014). Specifically, we

used Bayes factors (BFs) to evaluate the strength and consistency of our findings across verbal and spatial memory tasks. BF provides a powerful metric for comparing the likelihood of the observed data under different hypotheses, offering a rigorous measure of the evidence supporting the replication of effects. This analysis allowed us to provide a comprehensive assessment of the generalizability of our findings.

Our study offers new insights into the neurophysiological mechanisms that govern memory formation, specifically highlighting the role of hippocampal-parietal cortex interactions in both memory encoding and recall. Crucially, the robustness and generalizability of our findings were confirmed through their replication across three distinct experiments spanning the verbal and spatial memory domains.

Results

Causal information flow from the hippocampus to the parietal cortex in the VFR task

We first examined directed information flow from the hippocampus to the dorsal and ventral subdivisions of the PPC on the lateral surface, and the PCC/precuneus on the medial surface, during the memory encoding and recall periods of the VFR task. Participants were presented with a sequence of words and asked to remember them for subsequent recall (**Methods**, **Tables S1, S2a, S3a**, **Figure 1a**). Based on availability of sufficient electrode pairs in five or more study participants (see **Methods**), we demarcated two distinct subdivisions in the PPC: a dorsal PPC region encompassing the intraparietal sulcus, superior parietal lobule, and supramarginal gyrus and the ventral PPC encompassing the angular gyrus. There were insufficient electrodes pairs for more fine-grained connectivity analysis, we therefore combined electrodes from the superior parietal lobule, intraparietal sulcus, and supramarginal gyrus into a dorsal PPC subdivision and the angular gyrus regions into a ventral PPC subdivision. Briefly, the task consisted of three periods: encoding, delay, and recall (Solomon et al., 2019). During encoding, a list of 12 words was visually presented for ~30 sec. Each word was presented for a duration of 1600 msec, followed by an inter-stimulus interval of 800 to 1200 msec. After a 20 sec post-encoding delay, participants were instructed to recall as many words as possible during the 30 sec recall period.

Encoding We used phase transfer entropy (PTE) (Lobier et al., 2014) to compute broadband (0.5-160 Hz) causal influence from the hippocampus to dorsal PPC, ventral PPC, and PCC/precuneus and vice-versa. During memory encoding, the hippocampus had higher broadband causal influences on dPPC ($F(1, 392) = 339.21$, $p<0.001$, Cohen's $d = 1.86$), vPPC ($F(1, 130) = 26.45$, $p<0.001$, Cohen's $d = 0.90$), and PCC/precuneus ($F(1, 94) = 43.24$, $p<0.001$, Cohen's $d = 1.36$) than the reverse (**Figure 2a**).

Recall During memory recall, the hippocampus had higher broadband causal influences on dPPC ($F(1, 392) = 246.52$, $p<0.001$, Cohen's $d = 1.59$), vPPC ($F(1, 130) = 18.76$, $p<0.001$, Cohen's $d = 0.76$), and PCC/precuneus ($F(1, 94) = 14.45$, $p<0.001$, Cohen's $d = 0.79$) than the reverse (**Figure 2a**).

These results demonstrate that the hippocampus has higher directed causal information flow to the parietal cortex than the reverse, during both memory encoding and recall in the VFR task.

Differential causal information flow from the hippocampus to dPPC, vPPC, and PCC/precuneus in the VFR task

Encoding We next examined the differential causal information flow from the hippocampus to dPPC, vPPC, and PCC/precuneus. Causal influence of the hippocampus on dPPC, vPPC, and PCC/precuneus did not differ from each other during memory encoding (ps>0.05, Cohen's d < 0.31). Moreover, causal influence of dPPC, vPPC, and PCC/precuneus on the hippocampus did not differ from each other during memory encoding (ps>0.05, Cohen's d < 0.28).

Recall Causal influence of the hippocampus on dPPC and vPPC did not differ from each other during memory recall ($F(1, 272) = 0.05$, p>0.05, Cohen's $d = 0.00$). Causal influence of the hippocampus on vPPC and PCC/precuneus also did not differ from each other during memory recall ($F(1, 122) = 3.47$, p>0.05, Cohen's $d = 0.34$). Causal influence of the hippocampus on dPPC was higher than the causal influence of the hippocampus on PCC/precuneus during memory recall ($F(1, 245) = 18.54$, p<0.001, Cohen's $d = 0.55$). Furthermore, causal influence of dPPC, vPPC, and PCC/precuneus on the hippocampus did not differ from each other during memory recall (ps>0.05, Cohen's d < 0.25).

These results suggest equally strong directed information flow between the hippocampus and the lateral and medial regions of the parietal cortex in the VFR task.

Causal information flow from the hippocampus to the parietal cortex in the CATVFR task

We next examined directed information flow from the hippocampus to the dPPC, vPPC, and PCC/precuneus during the memory encoding and recall periods of the categorized verbal free recall task. In the CATVFR task, participants were presented with a list of words with consecutive pairs of words from a specific category (for example, JEANS-COAT, GRAPE-PEACH, etc.) and subsequently asked to recall as many as possible from the original list (**Methods**, **Tables S1, S2b, S3b**, **Figure 1b**) (Qasim, Mohan, Stein, & Jacobs, 2023). Similar to the uncategorized verbal free recall task, this task also consisted of three periods: encoding, delay, and recall. During encoding, a list of 12 words was visually presented for ~30 sec. Each word was presented for a duration of 1600 msec, followed by an inter-stimulus interval of 750 to 1000 msec. After a 20 sec post-encoding delay, participants were instructed to recall as many words as possible during the 30 sec recall period.

Encoding During memory encoding, the hippocampus had higher broadband causal influences on dPPC ($F(1, 197) = 165.47$, p<0.001, Cohen's $d = 1.83$), vPPC ($F(1, 92) = 7.72$, p<0.01, Cohen's $d = 0.58$), and PCC/precuneus ($F(1, 57) = 31.15$, p<0.001, Cohen's $d = 1.47$) than the reverse (**Figure 2b**).

Recall During memory recall, the hippocampus had higher broadband causal influences on dPPC ($F(1, 198) = 156.83$, p<0.001, Cohen's $d = 1.78$), vPPC ($F(1, 92) = 6.95$, p<0.01, Cohen's $d = 0.55$), and PCC/precuneus ($F(1, 58) = 37.57$, p<0.001, Cohen's $d = 1.61$) than the reverse (**Figure 2b**).

These results demonstrate that the hippocampus has higher directed information flow to the parietal cortex than the reverse, during both memory encoding and recall in the CATVFR task.

Differential causal information flow from the hippocampus to dPPC, vPPC, and PCC/precuneus in the CATVFR task

Encoding We examined the differential causal information flow from the hippocampus to dPPC, vPPC, and PCC/precuneus in the categorized verbal free recall task. Causal influence of the hippocampus on dPPC was higher than the causal influence of the hippocampus on vPPC during memory encoding ($F(1, 147) = 13.91$, $p<0.01$, Cohen's $d = 0.61$). Causal influence of the hippocampus on dPPC and PCC/precuneus did not differ from each other during memory encoding ($F(1, 127) = 0.48$, $p>0.05$, Cohen's $d = 0.12$). Causal influence of the hippocampus on vPPC and PCC/precuneus also did not differ from each other during memory encoding ($F(1, 68) = 2.56$, $p>0.05$, Cohen's $d = 0.39$). Moreover, causal influence of dPPC, vPPC, and PCC/precuneus on the hippocampus did not differ from each other during memory encoding (*ps*>0.05, Cohen's $d < 0.39$).

Recall Causal influence of the hippocampus on dPPC was higher than the causal influence of the hippocampus on vPPC during memory recall ($F(1, 148) = 17.94$, $p<0.01$, Cohen's $d = 0.70$). Causal influence of the hippocampus on dPPC and PCC/precuneus did not differ from each other during memory recall ($F(1, 126) = 0.07$, $p>0.05$, Cohen's $d = 0.05$). Causal influence of the hippocampus on vPPC and PCC/precuneus also did not differ from each other during memory recall ($F(1, 50) = 0.58$, $p>0.05$, Cohen's $d = 0.22$). Moreover, causal influence of dPPC, vPPC, and PCC/precuneus on the hippocampus did not differ from each other during memory recall (*ps*>0.05, Cohen's $d < 0.48$).

These results suggest higher directed information flow from the hippocampus to the dPPC compared to the vPPC in the CATVFR task.

Causal information flow from the hippocampus to the parietal cortex in the WMSM task

We next examined dynamic causal influences of the hippocampus on the parietal cortex in the water maze spatial memory task. In this task (**Methods**, **Tables S1, S2c, S3c**, **Figure 1c**), participants performed multiple trials of a spatial memory task in a virtual navigation paradigm (Goyal et al., 2018; Jacobs et al., 2016; Lee et al., 2018) similar to the Morris water maze (Morris, 1984). Participants were shown objects in various locations during the encoding periods and asked to retrieve the location of the objects during the recall period.

Encoding During spatial memory encoding, the hippocampus had higher broadband causal influences on dPPC ($F(1, 200) = 86.07$, $p<0.001$, Cohen's $d = 1.31$), vPPC ($F(1, 32) = 12.38$, $p<0.01$, Cohen's $d = 1.24$), and PCC/precuneus ($F(1, 57) = 20.54$, $p<0.001$, Cohen's $d = 1.20$) than the reverse (**Figures 2c**).

Recall We next examined causal influences of the hippocampus on the parietal cortex during the recall phase of the spatial memory task (**Figure 2c**, **Methods**). During spatial memory recall, the hippocampus had higher broadband causal influences on dPPC ($F(1, 200) = 83.67$, $p<0.001$,

Cohen's d = 1.29), vPPC ($F(1, 29) = 10.25$, $p<0.01$, Cohen's d = 1.19), and PCC/precuneus ($F(1, 56) = 10.35$, $p<0.01$, Cohen's d = 0.86) than the reverse (**Figures 2c**).

These results demonstrate that the hippocampus has higher directed causal information flow to the parietal cortex than the reverse, during both memory encoding and recall in the spatial memory task.

Differential causal information flow from the hippocampus to dPPC, vPPC, and PCC/precuneus in the WMSM task

Encoding Causal influence of the hippocampus on dPPC and vPPC did not differ from each other during memory encoding ($F(1, 121) = 1.73$, $p>0.05$, Cohen's d = 0.24). Causal influence of the hippocampus on both dPPC and vPPC were higher than the causal influence of the hippocampus on the PCC/precuneus during memory encoding ($F(1, 132) = 23.35$, $p<0.001$, Cohen's d = 0.84 and $F(1, 46) = 6.99$, $p<0.05$, Cohen's d = 0.78 respectively). Causal influence of dPPC and vPPC on the hippocampus did not differ from each other during memory encoding ($F(1, 118) = 4.67$, $p>0.05$, Cohen's d = 0.40). Causal influence of vPPC and PCC/precuneus on the hippocampus also did not differ from each other during memory encoding ($F(1, 48) = 1.20$, $p>0.05$, Cohen's d = 0.32). However, causal influence of the dPPC on the hippocampus was higher than the causal influence of the PCC/precuneus on the hippocampus during memory encoding ($F(1, 131) = 8.13$, $p<0.05$, Cohen's d = 0.50).

Recall Causal influence of the hippocampus on dPPC and vPPC did not differ from each other during memory recall ($F(1, 120) = 1.10$, $p>0.05$, Cohen's d = 0.19). Causal influence of the hippocampus on both dPPC and vPPC were higher than the causal influence of the hippocampus on the PCC/precuneus during memory recall ($F(1, 132) = 24.56$, $p<0.001$, Cohen's d = 0.86 and $F(1, 47) = 8.98$, $p<0.05$, Cohen's d = 0.88 respectively). Furthermore, causal influence of dPPC, vPPC, and PCC/precuneus on the hippocampus did not differ from each other during memory recall ($ps>0.05$, Cohen's $d < 0.29$).

Causal information flow from the hippocampus to the parietal cortex in the delta-theta frequency band in the VFR task

Based on previous findings from iEEG studies which have reported significant delta-theta frequency (0.5-8 Hz) band activity in the hippocampus during recall of information from recently encoded memories (Ekstrom & Watrous, 2014; Watrous et al., 2013) and based on our recent findings where we found higher directed information flow from the hippocampus to the prefrontal cortex than the reverse, in delta-theta frequency band during both encoding and recall, and across verbal and spatial episodic memory domains (Das & Menon, 2021, 2022b), we next investigated the dynamic causal influences of the hippocampus on dPPC, vPPC, and PCC/precuneus and vice-versa in the low frequency delta-theta (0.5-8 Hz) band. We computed PTE from dPPC, vPPC, PCC/precuneus to the hippocampus and, in the reverse direction, during episodic memory encoding, and recall in the delta-theta band in the verbal free recall task. This analysis revealed that the hippocampus had higher causal influences on dPPC ($F(1, 390) = 142.23$, $p<0.001$, Cohen's d = 1.21 for encoding and $F(1, 390) = 191.91$, $p<0.001$, Cohen's d = 1.40 for recall), vPPC ($F(1, 130) = 69.65$, $p<0.001$, Cohen's d = 1.47 for encoding and $F(1, 130)$

= 70.70, $p<0.001$, Cohen's $d = 1.48$ for recall), and PCC/precuneus ($F(1, 93) = 72.97$, $p<0.001$, Cohen's $d = 1.77$ for encoding and $F(1, 93) = 45.80$, $p<0.001$, Cohen's $d = 1.40$ for recall) than the reverse, during both memory encoding and recall conditions (**Figure 3a**).

These results demonstrate a key role for delta-theta frequency signaling underlying feedforward causal influences of the hippocampus on the parietal cortex in the VFR task.

Causal information flow from the hippocampus to the parietal cortex in the delta-theta frequency band in the CATVFR task

We next investigated the dynamic causal influences of the hippocampus on dPPC, vPPC, and PCC/precuneus and vice-versa in the delta-theta frequency band in the CATVFR task. This analysis revealed that the hippocampus had higher causal influences on dPPC ($F(1, 196) = 24.51$, $p<0.001$, Cohen's $d = 0.71$ for encoding and $F(1, 195) = 44.30$, $p<0.001$, Cohen's $d = 0.95$ for recall), vPPC ($F(1, 83) = 44.08$, $p<0.001$, Cohen's $d = 1.45$ for encoding and $F(1, 89) = 55.81$, $p<0.001$, Cohen's $d = 1.58$ for recall), and PCC/precuneus ($F(1, 57) = 35.86$, $p<0.001$, Cohen's $d = 1.59$ for encoding and $F(1, 57) = 53.37$, $p<0.001$, Cohen's $d = 1.93$ for recall) than the reverse, during both memory encoding and recall conditions (**Figure 3b**).

These results demonstrate a key role for delta-theta frequency signaling underlying feedforward causal influences of the hippocampus on the parietal cortex in the categorized verbal episodic memory task.

Causal information flow from the hippocampus to the parietal cortex in the delta-theta frequency band in the WMSM task

Similar to the verbal free recall tasks, this analysis revealed that the hippocampus had higher causal influences on dPPC ($F(1, 200) = 184.16$, $p<0.001$, Cohen's $d = 1.92$ for encoding and $F(1, 200) = 168.21$, $p<0.001$, Cohen's $d = 1.83$ for recall), vPPC ($F(1, 32) = 17.63$, $p<0.001$, Cohen's $d = 1.48$ for encoding and $F(1, 33) = 16.94$, $p<0.001$, Cohen's $d = 1.44$ for recall), and PCC/precuneus ($F(1, 56) = 199.58$, $p<0.001$, Cohen's $d = 3.76$ for encoding and $F(1, 57) = 160.71$, $p<0.001$, Cohen's $d = 3.36$ for recall) than the reverse, during both spatial memory encoding and recall conditions (**Figure 3c**).

Replication of same results in the delta-theta frequency band during the spatial memory task emphasize a key role for delta-theta frequency signaling underlying feedforward causal influences of the hippocampus on the parietal cortex across multiple memory domains.

Causal information flow from the parietal cortex to the hippocampus in the beta frequency band in the VFR task

Next, we examined directed information flow between the hippocampus and parietal cortex in the beta frequency (12-30 Hz) band based on emerging findings in non-human primates regarding cortical signaling in the beta band during cognition (Engel & Fries, 2010) and based on our recent findings where we found higher directed information flow from the prefrontal cortex to the hippocampus than the reverse, in beta frequency band during both encoding and recall, and

across verbal and spatial episodic memory domains (Das & Menon, 2021, 2022b). We computed PTE from the parietal cortex nodes to the hippocampus, and in the reverse direction, during encoding and recall in the beta frequency band in the verbal free recall task. This analysis revealed that dPPC ($F(1, 391) = 328.5$, $p<0.001$, Cohen's $d = 1.83$ for encoding and $F(1, 392) = 277.12$, $p<0.001$, Cohen's $d = 1.68$ for recall), vPPC ($F(1, 129) = 167.3$, $p<0.001$, Cohen's $d = 2.28$ for encoding and $F(1, 129) = 186.1$, $p<0.001$, Cohen's $d = 2.40$ for recall), and PCC/precuneus ($F(1, 92) = 40.78$, $p<0.001$, Cohen's $d = 1.33$ for encoding and $F(1, 92) = 6.25$, $p<0.05$, Cohen's $d = 0.52$ for recall) had higher causal influences on the hippocampus than the reverse, during both memory encoding and recall conditions (**Figure 4a**).

These results demonstrate a key role for beta frequency signaling underlying feedback causal influences of the parietal cortex on the hippocampus in the verbal free recall task.

Causal information flow from the parietal cortex to the hippocampus in the beta frequency band in the CATVFR task

We next examined directed information flow between the hippocampus and parietal cortex in the beta frequency band in the CATVFR task. This analysis revealed that dPPC ($F(1, 196) = 159.74$, $p<0.001$, Cohen's $d = 1.81$ for encoding and $F(1, 197) = 65.04$, $p<0.001$, Cohen's $d = 1.15$ for recall), vPPC ($F(1, 98) = 142.37$, $p<0.001$, Cohen's $d = 2.41$ for encoding and $F(1, 98) = 114.09$, $p<0.001$, Cohen's $d = 2.16$ for recall), and PCC/precuneus ($F(1, 57) = 29.49$, $p<0.001$, Cohen's $d = 1.44$ for encoding and $F(1, 57) = 6.51$, $p<0.05$, Cohen's $d = 0.67$ for recall) had higher causal influences on the hippocampus than the reverse, during both memory encoding and recall conditions (**Figure 4b**).

These results demonstrate a key role for beta frequency signaling underlying feedback causal influences of the parietal cortex on the hippocampus in the categorized verbal free recall task.

Causal information flow from the parietal cortex to the hippocampus in the beta frequency band in the WMSM task

Similar to the verbal free recall tasks, this analysis revealed that dPPC ($F(1, 198) = 285.43$, $p<0.001$, Cohen's $d = 2.40$ for encoding and $F(1, 200) = 234.83$, $p<0.001$, Cohen's $d = 2.17$ for recall), vPPC ($F(1, 32) = 73.29$, $p<0.001$, Cohen's $d = 3.01$ for encoding and $F(1, 32) = 61.55$, $p<0.001$, Cohen's $d = 2.79$ for recall), and PCC/precuneus ($F(1, 56) = 7.39$, $p<0.01$, Cohen's $d = 0.73$ for encoding and $F(1, 54) = 20.03$, $p<0.001$, Cohen's $d = 1.22$ for recall) had higher causal influences on the hippocampus than the reverse, during both spatial memory encoding and recall conditions (**Figure 4c**).

Replication of same results in the beta frequency band during the spatial memory task recapitulate a key role for beta frequency signaling underlying feedback causal influences of the parietal cortex on the hippocampus across multiple memory domains.

Replication of causal directed information flow between the hippocampus and the parietal cortex across memory domains

We used replication BF analysis to estimate the degree of replicability of direction of information flow across multiple tasks and domains (**Table 1**). Specifically, we used the posterior distribution obtained from the VFR (original) dataset as a prior distribution for the test of data from the CATVFR and WMSM (replication) datasets (Ly et al., 2019) (see **Methods** for details).

Encoding We first used replication BF analysis for the encoding phase of the memory tasks (**Table 1a**). Findings corresponding to the direction of information flow between the hippocampus and the dPPC during memory encoding were replicated in the broadband across tasks (BFs 7.61e+35 and 3.84e+16 for CATVFR and WMSM respectively). Findings corresponding to the direction of information flow between the hippocampus and vPPC during memory encoding were also replicated in the broadband across tasks (BFs 5.91e+0 and 3.84e+16 for CATVFR and WMSM respectively). Furthermore, findings corresponding to the direction of information flow between the hippocampus and PCC/precuneus were also replicated across tasks (BFs 1.04e+4 and 4.67e+0 for CATVFR and WMSM respectively).

These results demonstrate very high replicability of directed information flow from the hippocampus to the parietal cortex nodes in broadband, during memory encoding.

Recall We next repeated the replication BF analysis for the recall periods of the memory tasks (**Table 1b**). Findings corresponding to the direction of information flow between the hippocampus and the dPPC during memory recall were replicated across tasks (BFs 6.78e+36 and 1.42e+14 for CATVFR and WMSM respectively). Findings corresponding to the direction of information flow between the hippocampus and vPPC during memory recall were also replicated across tasks (BFs 1.54e+1 and 9.61e+0 for CATVFR and WMSM respectively). Furthermore, findings corresponding to the direction of information flow between the hippocampus and PCC/precuneus were also replicated across tasks (BFs 2.77e+4 and 6.13e+1 for CATVFR and WMSM respectively).

These results demonstrate very high replicability of directed information flow from the hippocampus to the parietal cortex nodes in broadband, during memory recall.

Replication of causal directed information flow between the hippocampus and the parietal cortex across memory domains in the delta-theta and beta frequency bands

We next repeated the replication BF analysis to estimate the degree of replicability of direction of information flow across multiple tasks and memory domains in the delta-theta and beta frequency bands (**Table 1**).

Encoding Findings corresponding to the direction of information flow between the hippocampus and the dPPC (BFs 1.58e+4 and 8.73e+33 for CATVFR and WMSM respectively), vPPC (BFs 1.44e+5 and 1.85e+2 for CATVFR and WMSM respectively), and PCC/precuneus (BFs 9.46e+8 and 1.61e+16 for CATVFR and WMSM respectively) during memory encoding were replicated

in the delta-theta band across tasks (**Table 1a**). Similarly, findings corresponding to the direction of information flow between the hippocampus and the dPPC (BFs 1.47e+30 and 5.05e+34 for CATVFR and WMSM respectively) and vPPC (BFs 2.53e+16 and 2.36e+7 for CATVFR and WMSM respectively) were also replicated in the beta band across tasks (**Table 1a**). Findings corresponding to the direction of information flow between the hippocampus and the PCC/precuneus was replicated for the CATVFR task in the beta band (BF 6.64e+5) (**Table 1a**).

Recall Findings corresponding to the direction of information flow between the hippocampus and the dPPC (BFs 1.38e+12 and 1.55e+31 for CATVFR and WMSM respectively), vPPC (BFs 4.29e+8 and 9.88e+1 for CATVFR and WMSM respectively), and PCC/precuneus (BFs 9.55e+8 and 7.31e+12 for CATVFR and WMSM respectively) during memory recall were replicated in the delta-theta band across tasks (**Table 1b**). Similarly, findings corresponding to the direction of information flow between the hippocampus and the dPPC (BFs 3.56e+13 and 6.65e+28 for CATVFR and WMSM respectively), vPPC (BFs 7.32e+11 and 1.99e+8 for CATVFR and WMSM respectively), and PCC/precuneus (BFs 8.19e+1 and 3.88e+1 for CATVFR and WMSM respectively) during memory recall were also replicated in the beta band across tasks (**Table 1b**).

Together, these results demonstrate very high replicability of directed information flow between the hippocampus and the parietal cortex nodes in delta-theta and beta frequency bands, during both memory encoding and recall.

Surrogate data analysis of causal information flow between the hippocampus and the parietal cortex

Next, we conducted surrogate data analysis to test the significance of the estimated PTE values compared to PTE expected by chance (**Methods**). The estimated phases from the Hilbert transform for electrodes from pairs of brain areas were time-shuffled and PTE analysis was repeated on this shuffled data to build a distribution of surrogate PTE values against which the observed PTE was tested. This analysis revealed that causal directed information flow from the hippocampus to the dPPC was significantly higher than those expected by chance in broadband during memory encoding in the VFR task ($p<0.05$). Causal directed information flow from the hippocampus to the dPPC was also significantly higher than those expected by chance in broadband during both encoding and recall in the WMSM task ($ps<0.05$).

Frequency-specific surrogate data analysis further revealed that causal information flow from the hippocampus to the dorsal and ventral subdivisions of the PPC and the PCC/precuneus and the reverse were significantly higher than those expected by chance ($p<0.05$ in all cases) in the delta-theta frequency band for both memory encoding and recall conditions, and across verbal free recall, categorized verbal free recall, and water maze spatial memory tasks, indicating bidirectional causal information flow between the hippocampus and the parietal cortex in delta-theta band. Analysis in the beta, gamma, and high-gamma frequency bands revealed that causal information flow from the hippocampus to dPPC, vPPC and PCC/precuneus and the reverse were significantly lower than those expected by chance ($p<0.05$ in all cases) for both memory encoding and recall conditions and across verbal free recall, categorized verbal free recall, and water maze spatial memory tasks, indicating significantly lower predictability of one brain area from the other than expected by chance, in these frequency bands.

These results demonstrate that most reported effects in this study arise from causal signaling that is significantly beyond chance levels.

Task-related high-gamma power in hippocampus compared to dorsal and ventral PPC, and PCC/precuneus during encoding and recall

We next examined neuronal activity in the hippocampus and the dorsal PPC, ventral PPC, and PCC/precuneus and tested whether activity in the PCC/precuneus is suppressed compared to activity in the hippocampus. Previous studies have suggested that power in the high gamma band (80-160 Hz) is correlated with fMRI BOLD signals (Hutchison, Hashemi, Gati, Menon, & Everling, 2015; Lakatos, Gross, & Thut, 2019; Leopold, Murayama, & Logothetis, 2003; Mantini, Perrucci, Del Gratta, Romani, & Corbetta, 2007; Scholvinck, Maier, Ye, Duyn, & Leopold, 2010), and is thought to reflect local neuronal activity (Canolty & Knight, 2010). Therefore, we compared high-gamma power (**Methods**) in the hippocampus with the dorsal and ventral subdivisions of the PPC and the PCC/precuneus during memory encoding and recall conditions across verbal and spatial episodic memory domains.

This analysis revealed that high-gamma power in the PCC/precuneus was suppressed compared to high-gamma power in the hippocampus almost throughout the encoding periods of the verbal free recall, categorized verbal free recall, and water maze spatial memory tasks ($ps<0.05$) (**Figures 5a-c**). High-gamma power results during the recall periods were not consistent across the three tasks (**Figures 5a-c**). Moreover, high-gamma power of the hippocampus compared to those from the dorsal or ventral PPC was also not consistent across the three tasks (**Figures 5a-c**).

Discussion

We examined the electrophysiological basis of directed information flow between the hippocampus and the parietal cortex during encoding and recall and across verbal and spatial episodic memory processing in humans using iEEG recordings from a robust sample of 98 participants. Our analysis first focused on directed information flow in broadband, as investigations using canonically defined frequency bands can miss aperiodic (1/f) components which can have major influence on causal signaling between brain regions (Canales-Johnson et al., 2021; Donoghue et al., 2020). Direction-specific information theoretic analysis revealed that the hippocampus has higher causal influence on the parietal cortex than the reverse, and crucially, this pattern was observed during both the encoding and recall phases and across verbal and spatial memory domains. Our analysis further revealed frequency specificity of hippocampus-parietal cortex interactions and a dissociation between feedforward and feedback information flow in the delta-theta and beta frequency bands. Our findings provide novel insights into asymmetric directed of information flow between the hippocampus and the parietal cortex during verbal and spatial memory formation in the human brain (**Figure 6**).

Our analysis of causal signaling was based on phase transfer entropy (PTE), which provides a robust and powerful tool for characterizing information flow between brain regions based on phase coupling (Hillebrand et al., 2016; Lobier et al., 2014; M. Y. Wang et al., 2017). Previous

findings using multielectrode array recordings in both humans and animal models have established that phase, rather than amplitude, is crucial for both spatial and temporal encoding of information in the brain (Kayser, Montemurro, Logothetis, & Panzeri, 2009; Lachaux, Rodriguez, Martinerie, & Varela, 1999; Lopour, Tavassoli, Fried, & Ringach, 2013; Ng, Logothetis, & Kayser, 2013; Siegel, Warden, & Miller, 2009). PTE assesses with the ability of one time-series to predict future values of another time-series thus estimating the time-delayed causal influences between the two time-series. Crucially, PTE is a robust, nonlinear measure of directionality of information flow between time-series (Das, de Los Angeles, & Menon, 2022; Das & Menon, 2020, 2021, 2022a, 2022b, 2023; Hillebrand et al., 2016; Lobier et al., 2014).

PTE revealed significantly higher broadband causal influence of the hippocampal electrodes on the parietal cortex electrodes than the reverse, during both encoding and recall of memory. Crucially, this asymmetric pattern of directed causal information flow was replicated across both verbal and spatial memory tasks. These findings build upon our recent iEEG findings where we have shown replicable pattern of directed information flow from the hippocampus to the middle frontal gyrus and inferior frontal gyrus subdivisions of the prefrontal cortex than the reverse, during memory encoding and recall and across verbal and spatial memory domains (Das & Menon, 2021, 2022b). The current findings thus suggest that the hippocampus has directed causal influence on broad cortical areas involving both the prefrontal and parietal cortices. Our findings also converge on recent findings from iEEG recordings in humans that have shown that the left hemisphere hippocampus plays a crucial role for episodic and spatial memory processing (Ekstrom et al., 2005; Gonzalez et al., 2015). Furthermore, recent iEEG studies involving intracranial stimulation of the bilateral medial temporal lobe suggest that directed information flow between hippocampus and parietal cortex contributes to successful memory retrieval (Das & Menon, 2023). Findings are also consistent with previous multiple structural and functional MRI (Grön, Wunderlich, Spitzer, Tomczak, & Riepe, 2000; Iglói, Doeller, Berthoz, Rondi-Reig, & Burgess, 2010; Kaplan, Horner, Bandettini, Doeller, & Burgess, 2014; Maguire, Burgess, & O'Keefe, 1999; Maguire et al., 2000), positron imaging tomography (PET) (Ghaem et al., 1997; Maguire et al., 1998; Maguire et al., 1999), and magnetoencephalography (MEG) (Pu, Cornwell, Cheyne, & Johnson, 2017) studies in humans which have revealed the involvement of bilateral hippocampus in spatial navigation and memory. Our findings thus provide robust electrophysiological evidence for dynamic causal influence of the left hippocampus on both the lateral and medial parietal cortex during both verbal and spatial episodic memory encoding and recall.

We focused on dynamic interactions between the left hemisphere hippocampus and the parietal cortex. This focus was necessitated by the limitation that our iEEG data had inadequate coverage in the right hippocampus. While the left hemisphere hippocampus is widely recognized for its dominant role in verbal episodic memory encoding and recall (Burgess et al., 2002), its role in spatial memory processing has remained poorly understood. The contribution of the left hemisphere to spatial memory is less clear, although some studies point to the involvement of both the left and right hippocampi (Bohbot et al., 1998; Maguire et al., 1996; Spiers et al., 2001). These findings are supported by structural and functional MRI, PET, MEG, and iEEG studies, which have also implicated both the left and right hippocampi in spatial navigation and memory (Bohbot et al., 1998; Maguire, Burke, Phillips, & Staunton, 1996; Spiers et al., 2001).

iEEG studies in humans have also pointed to the involvement of both the left and right hemisphere hippocampus in spatial navigation and memory (J. Miller et al., 2018; Stangl et al., 2021).

Importantly, our findings of left hippocampal causal signaling during both verbal and spatial memory aligns with recent work by Seger and colleagues, which suggests that memory might be a more potent driver of hippocampal theta oscillations in humans than navigation (Seger, Kriegel, Lega, & Ekstrom, 2023). In their study, patients who mentally simulated routes they had just navigated showed greater hippocampal theta power, higher frequency, and longer duration of oscillations than during actual navigation. This suggests that in humans, unlike in rodents, memory might be a more potent catalyst for hippocampal theta oscillations. These findings support models of internally generated theta oscillations in the human hippocampus and could indicate that memory, rather than spatial navigation, is the primary function driving hippocampal activity (Ekstrom & Hill, 2023). In our study, the focus on the left hemisphere, which is traditionally associated predominantly with verbal memory, assumes greater relevance in light of these new findings. It raises the possibility that the left hippocampus may play a more comprehensive role in memory-related processes, extending beyond verbal tasks to encompass spatial memory tasks as well.

The PCC/precuneus and the ventral PPC, two key nodes of the DMN, are typically deactivated during attention demanding tasks (Wen, Liu, Yao, & Ding, 2013). Despite this, they are directly implicated in episodic memory functions (Buckner et al., 2008; Menon, 2023). In contrast, the dorsal PPC, a central node of the frontoparietal control network and integral to cognitive control over memory, typically displays heightened activity during memory tasks (Badre, Poldrack, Paré-Blagoev, Insler, & Wagner, 2005; Badre & Wagner, 2007; Wagner, Paré-Blagoev, Clark, & Poldrack, 2001; Wagner et al., 2005). Our high-resolution iEEG analysis revealed that, specifically during encoding, high-gamma power was consistently suppressed in the PCC/precuneus relative to the hippocampus across all three episodic memory experiments. This suppression was unique to the PCC/precuneus; no such pattern emerged in either the dorsal or ventral PPC. Our findings significantly extend this knowledge base to specific phases of memory formation, leveraging high-resolution iEEG recordings for temporal precision. Importantly, even though the hippocampus and the PCC/precuneus are both associated with the DMN, we observed a clear dissociation of high-gamma dynamics between these two brain areas. The PCC/precuneus high-gamma activity was suppressed compared to the hippocampus during encoding, and both brain regions were similarly active during the recall periods of the tasks, suggesting context-specific dissociation between these DMN nodes.

Contrary to our initial predictions regarding the ventral PPC's alignment with the DMN, we found that neural responses in this region were not suppressed compared to the hippocampus during either encoding or recall. Instead, the ventral PPC displayed heightened neural activity, similar to what we observed in the dorsal PPC. One explanation may lie in the functional heterogeneity of the ventral PPC, particularly the angular gyrus, which has distinct cytoarchitectonic subregions – PGa and PGp – with divergent functional roles (Bellana, Ladyka-Wojcik, Lahan, Moscovitch, & Grady, 2023; Niu & Palomero-Gallagher, 2023; Rockland & Graves, 2023; Uddin et al., 2010; Wu et al., 2009). The former appears aligned with the dorsal PPC and the frontoparietal network, while the latter is more closely associated with the DMN

(Seghier, 2013, 2023; Seghier, Fagan, & Price, 2010). Future research with adequate subregion sampling is necessary to resolve questions around this functional heterogeneity and its alignment with the DMN.

High-gamma (80-160 Hz) activity is a reliable indicator of localized neuronal activity, with observed elevations during a variety of cognitive tasks including working memory and episodic memory (Canolty et al., 2006; Crone, Boatman, Gordon, & Hao, 2001; Daitch & Parvizi, 2018; Edwards, Soltani, Deouell, Berger, & Knight, 2005; Lachaux et al., 2005; Mainy et al., 2007; Sederberg et al., 2007; Tallon-Baudry, Bertrand, Hénaff, Isnard, & Fischer, 2005). The observed suppression in high-gamma power in the PCC/precuneus compared to the hippocampus specifically during memory encoding, but not during recall, offers strong evidence for the selective functional downregulation of this region when processing external stimuli during the encoding phase of episodic memory formation. Interestingly, despite these patterns of local modulation in high-gamma power, our analysis found a substantial causal influence exerted by the hippocampus on both the lateral and medial parietal cortex across a broad frequency spectrum (0.5-160 Hz) as well as the low-frequency delta-theta (0.5-8 Hz) band. However, this causal influence was notably absent in the high-gamma frequency range (**Figures S1, S2**). This distinction aligns with current models positing that high-gamma activity is predominantly indicative of localized processing, whereas lower-frequency oscillations are more likely to mediate long-range network interactions (Bastos et al., 2015; Das et al., 2022; Das & Menon, 2020, 2021, 2022b, 2023; K. J. Miller et al., 2007). Our findings thus underscore the necessity of differentiating between high-gamma and broadband fluctuations, as these separate spectral domains reflect distinct physiological phenomena with specific roles in neural network function during episodic memory formation.

The second objective of our study was to investigate the frequency specificity of directional information flow between the hippocampus and the parietal cortex. Electrophysiological studies in rodents have reported strong delta (0.5-4 Hz), theta (4-8 Hz), and beta (12-30 Hz) frequency band oscillations in the hippocampus (Schultheiss et al., 2020; Trimper, Galloway, Jones, Mandi, & Manns, 2017; Trimper, Stefanescu, & Manns, 2014) and theta-gamma phase-amplitude coupling between the hippocampus and the PPC, with hippocampus-theta modulating gamma power in the PPC (Sirota et al., 2008). Based on previous reports in rodents, non-human primates, and humans, we focused on delta-theta (0.5-8 Hz) and beta (12-30 Hz), frequency bands, as enhanced local field potentials in these frequency bands have been identified in the hippocampus and parietal cortex (Ekstrom et al., 2005; Ekstrom & Watrous, 2014; Engel & Fries, 2010; Gonzalez et al., 2015; Watrous et al., 2013). In our previous iEEG studies, we have found higher directed information flow from the hippocampus to the prefrontal cortex than the reverse, in delta-theta frequency band and higher directed information flow from the prefrontal cortex to the hippocampus than the reverse, in beta frequency band, during both encoding and recall, and across verbal and spatial episodic memory domains (Das & Menon, 2021, 2022b). Moreover, previous iEEG studies have reported significant delta-theta frequency (0.5-8 Hz) band activity in the hippocampus during recall of spatial information from recently encoded memories (Goyal et al., 2018; Jacobs et al., 2016), but the common frequency-specificity of causal hippocampal-parietal cortex signaling in the human brain associated with verbal and spatial memory encoding and recall has not been well understood.

In the delta-theta band, we found that the hippocampus had higher causal influences on the parietal cortex, compared to the reverse direction; this pattern was observed during both memory encoding and recall periods and across verbal and spatial memory domains. This finding is consistent with reports of theta frequency band left hemisphere hippocampal-PPC synchronization during spatial memory tasks (Ekstrom et al., 2005). In contrast, we found an opposite pattern in the beta band with higher parietal cortex causal influences on the hippocampus, compared to the reverse direction; again, this pattern was observed during both memory encoding and recall periods and across verbal and spatial memory domains. Top-down information flow from the PPC in the beta-band may contribute to transitioning latent neuronal ensembles into "active" representations (Spitzer & Haegens, 2017) as well as the subsequent maintenance of information in cell assemblies (Engel & Fries, 2010), while delta-theta rhythms in the hippocampus may signal pattern completion associated with memory recall that is conveyed to multiple parietal cortex regions (Cabeza et al., 2008). In sum, these results suggest that the hippocampus and parietal cortex exert feedforward and feedback influences through distinct frequency channels and that delta-theta and beta rhythms have different synchronization properties. This frequency dependent directionality of information flow may putatively provide parallel signaling pathways between the hippocampus and the parietal cortex for verbal and spatial memory processing.

Finally, a major objective of our study was to replicate findings across verbal and spatial memory domains. Replication of findings is a major problem in neuroscience, particularly in iEEG studies involving multiple distributed brain areas where data sharing is virtually nonexistent and data are difficult to acquire spanning distributed brain regions (Das & Menon, 2022b). To estimate the degree of replicability of our findings across the verbal and spatial memory domains, we employed replication Bayes Factor (BF) analysis (Ly et al., 2019; Verhagen & Wagenmakers, 2014). We found very high replication BF related to the causal information flow between the hippocampus and the parietal cortex (**Table 1**), emphasizing the robustness of our findings – a challenging proposition in iEEG research. Furthermore, we discovered that most BFs associated with the replication of direction of information flow between the hippocampus and parietal cortex were decisive (BFs > 100), demonstrating consistent results across multiple memory domains and task contexts.

Our findings contribute new insights into the relatively understudied hippocampus-parietal circuits and their role in episodic memory. Remarkably, the patterns of causal information flow and frequency-specific interactions observed in this study parallel those we previously reported between the hippocampus and the prefrontal cortex (Das & Menon, 2022b). In both cases, we identified asymmetric information flow during memory encoding and recall periods. This consistency across distinct neural circuits suggests a potentially generalized mechanism for episodic memory formation in the human brain. The robustness of these results, demonstrated through Bayesian analysis, lends further credence to the pivotal role of hippocampus-parietal interactions in episodic memory. Therefore, our current study not only fills a gap in the existing literature but also corroborates and extends our understanding of the complex neural circuit dynamics underlying memory processes.

Conclusions

Our study advances foundational knowledge of directed information flow between the hippocampus and the parietal cortex during verbal and spatial memory formation in humans. Utilizing high temporal resolution iEEG recordings from a large cohort of participants and across multiple task domains, we uncovered distinct frequency-specific feedforward and feedback signaling mechanisms between the hippocampus and the parietal cortex. Our findings not only deepen our understanding of the neural architectures involved in both verbal and spatial memory but also lay groundwork for future studies aimed at exploring memory circuit dysfunctions prominent in psychiatric and neurological disorders. Moreover, our work has implications for future research and potential therapies, particularly those involving targeted stimulation of parietal cortex regions to indirectly modulate hippocampal activity (J. X. Wang et al., 2014). More broadly, our study serves as a reference for deciphering the dynamic electrophysiological interactions that govern complex cognitive functions.

Methods

UPENN-RAM iEEG recordings

iEEG recordings from 249 patients shared by Kahana and colleagues at the University of Pennsylvania (UPENN) (obtained from the UPENN-RAM public data release) were used for analysis (Jacobs et al., 2016). Patients with pharmaco-resistant epilepsy underwent surgery for removal of their seizure onset zones. iEEG recordings of these patients were downloaded from a UPENN-RAM consortium hosted data sharing archive (URL: http://memory.psych.upenn.edu/RAM). Prior to data collection, research protocols and ethical guidelines were approved by the Institutional Review Board at the participating hospitals and informed consent was obtained from the participants and guardians (Jacobs et al., 2016). Details of all the recordings sessions and data pre-processing procedures are described by Kahana and colleagues (Jacobs et al., 2016). Briefly, iEEG recordings were obtained using subdural grids and strips (contacts placed 10 mm apart) or depth electrodes (contacts spaced 5–10 mm apart) using recording systems at each clinical site. iEEG systems included DeltaMed XlTek (Natus), Grass Telefactor, and Nihon-Kohden EEG systems. Electrodes located in brain lesions or those which corresponded to seizure onset zones or had significant interictal spiking or had broken leads, were excluded from analysis.

Anatomical localization of electrode placement was accomplished by co-registering the postoperative computed CTs with the postoperative MRIs using FSL (FMRIB (Functional MRI of the Brain) Software Library), BET (Brain Extraction Tool), and FLIRT (FMRIB Linear Image Registration Tool) software packages. Preoperative MRIs were used when postoperative MRIs were not available. The resulting contact locations were mapped to MNI space using an indirect stereotactic technique and OsiriX Imaging Software DICOM viewer package. We used the Brainnetome atlas (Fan et al., 2016) to demarcate the left hemisphere dorsal and ventral subdivisions of the posterior parietal cortex (dPPC and vPPC), the hippocampus, and the posterior cingulate cortex (PCC)/precuneus (Cabeza et al., 2008; Hutchinson et al., 2009). We first identified electrode pairs in which there were at least five patients with electrodes implanted in each pair of brain regions of interest encompassing dPPC, vPPC, hippocampus, and PCC/precuneus. Key PPC regions of interest included the superior parietal lobule, supramarginal gyrus, and intraparietal sulcus and angular gyrus in the inferior parietal lobule, spanning its dorsal-ventral axis. The lack of sufficient number of participants and electrode pairs precluded analyses of these subdivisions separately. We therefore combined electrodes from the superior parietal lobule, intraparietal sulcus, and supramarginal gyrus into a dorsal PPC subdivision and the angular gyrus regions into a ventral PPC subdivision (**Tables S2, S3**). Out of 249 individuals, data from 98 individuals (aged from 18 to 64, mean age 38.2 ± 12.5, 53 females) were used for subsequent analysis based on electrode placement in dPPC, vPPC, hippocampus, and PCC/precuneus. Gender differences were not analyzed in this study due to lack of sufficient male participants for electrodes pairs for hippocampus-dPPC, hippocampus-vPPC, and hippocampus-PCC/precuneus interactions (**Table S2c**).

Original sampling rates of iEEG signals were 500 Hz, 1000 Hz, 1024 Hz, and 1600 Hz. Hence, iEEG signals were downsampled to 500 Hz, if the original sampling rate was higher, for all subsequent analysis. The two major concerns when analyzing interactions between closely spaced intracranial electrodes are volume conduction and confounding interactions with the

reference electrode (Burke et al., 2013). Hence bipolar referencing was used to eliminate confounding artifacts and improve the signal-to-noise ratio of the neural signals, consistent with previous studies using UPENN-RAM iEEG data (Burke et al., 2013; Ezzyat et al., 2018). Signals recorded at individual electrodes were converted to a bipolar montage by computing the difference in signal between adjacent electrode pairs on each strip, grid, and depth electrode and the resulting bipolar signals were treated as new "virtual" electrodes originating from the midpoint between each contact pair, identical to procedures in previous studies using UPENN-RAM data (Solomon et al., 2019). Line noise (60 Hz) and its harmonics were removed from the bipolar signals and finally each bipolar signal was Z-normalized by removing mean and scaling by the standard deviation. For filtering, we used a fourth order two-way zero phase lag Butterworth filter throughout the analysis.

iEEG verbal free recall and spatial memory tasks

(a) Verbal free recall task

Patients performed multiple trials of a "free recall" experiment, where they were presented with a list of words and subsequently asked to recall as many as possible from the original list (**Figure 1a**) (Solomon et al., 2017; Solomon et al., 2019). The task consisted of three periods: encoding, delay, and recall. During encoding, a list of 12 words was visually presented for ~30 sec. Words were selected at random, without replacement, from a pool of high frequency English nouns (http://memory.psych.upenn.edu/Word_Pools). Each word was presented for a duration of 1600 msec, followed by an inter-stimulus interval of 800 to 1200 msec. After a 20 sec post-encoding delay, participants were instructed to recall as many words as possible during the 30 sec recall period. Average recall accuracy across patients was 24.8% ± 9.7%, similar to prior studies of verbal episodic memory retrieval in neurosurgical patients (Burke et al., 2014). The mismatch in the number trials therefore made it difficult to directly compare causal signaling measures between successfully versus unsuccessfully recalled words. From the point of view of probing behaviorally effective memory encoding, our focus was therefore on successful encoding and recall consistent with most prior studies (Long, Burke, & Kahana, 2014; Watrous et al., 2013). We analyzed iEEG epochs from the encoding and recall periods of the free recall task. For the recall periods, iEEG recordings 1600 msec prior to the vocal onset of each word were analyzed (Solomon et al., 2019). Data from each trial was analyzed separately and specific measures were averaged across trials.

(b) Categorized verbal free recall task

This task was very similar to the verbal free recall task. Here, patients performed multiple trials of a "categorized free recall" experiment, where they were presented with a list of words with consecutive pairs of words from a specific category (for example, JEANS-COAT, GRAPE-PEACH, etc.) and subsequently asked to recall as many as possible from the original list (**Figure 1b**) (Qasim et al., 2023). Similar to the uncategorized verbal free recall task, this task also consisted of three periods: encoding, delay, and recall. During encoding, a list of 12 words was visually presented for ~30 sec. Semantic categories were chosen using Amazon Mechanical Turk. Pairs of words from the same semantic category were never presented consecutively. Each word was presented for a duration of 1600 msec, followed by an inter-stimulus interval of 750 to

1000 msec. After a 20 sec post-encoding delay, participants were instructed to recall as many words as possible during the 30 sec recall period. Average recall accuracy across patients was 27.0% ± 11.9%. Similar to the uncategorized verbal free recall task, we focused on trials corresponding to successful encoding and recall. Analysis of iEEG epochs from the encoding and recall periods of the categorized free recall task was same as the uncategorized verbal free recall task.

(c) Water maze spatial memory task

Participants performed multiple trials of a spatial memory task in a virtual navigation paradigm (Goyal et al., 2018; Jacobs et al., 2016; Lee et al., 2018) similar to the Morris water maze (Morris, 1984). The environment was rectangular (1.8:1 aspect ratio), and was surrounded by a continuous boundary (**Figure 1c**). There were four distal visual cues (landmarks), one centered on each side of the rectangle, to aid with orienting. Each trial (96 trials per session, 1–3 sessions per subject) started with two 5 sec *encoding periods*, during which subjects were driven to an object from a random starting location. At the beginning of an encoding period, the object appeared and, over the course of 5 sec, the subject was automatically driven directly toward it. The 5 sec period consisted of three intervals: first, the subject was rotated toward the object (1 sec), second, the subject was driven toward the object (3 sec), and, finally, the subject paused while at the object location (1 sec). After a 5 sec delay with a blank screen, the same process was repeated from a different starting location. After both encoding periods for each item, there was a 5 sec pause followed by the *recall period*. The subject was placed in the environment at a random starting location with the object hidden and then asked to freely navigate using a joystick to the location where they thought the object was located. When they reached their chosen location, they pressed a button to record their response. They then received feedback on their performance via an overhead view of the environment showing the actual and reported object locations. Average recall accuracy across patients was 48.6% ± 4.2%.

Similar to the verbal free recall task, only trials corresponding to successful memory encoding and recall are considered in our analysis. We analyzed 5 sec iEEG epochs from the encoding and recall periods of the task. Data from each trial was analyzed separately and specific measures were averaged across trials, similar to the verbal free recall task.

iEEG analysis of high-gamma power

We first filtered the signals in the high-gamma (80-160 Hz) frequency band (Raccah, Daitch, Kucyi, & Parvizi, 2018) and then calculated the square of the filtered signals as the power of the signals (Kwon et al., 2021). Signals were then smoothed using 0.2s windows with 90% overlap (Kwon et al., 2021) and normalized with respect to 0.2s pre-stimulus periods.

iEEG analysis of phase transfer entropy (PTE) and causal dynamics

Phase transfer entropy (PTE) is a nonlinear measure of the directionality of information flow between time-series and can be applied as a measure of causality to nonstationary time-series (Lobier et al., 2014). Note that information flow described here relates to signaling between brain areas and does not necessarily reflect the representation or coding of behaviorally relevant

variables per se. The PTE measure is in contrast to the Granger causality measure which can be applied only to stationary time-series (Barnett & Seth, 2014). We first carried out a stationarity test of the iEEG recordings (unit root test for stationarity (Barnett & Seth, 2014)) and found that the spectral radius of the autoregressive model is very close to one, indicating that the iEEG time-series is nonstationary. This precluded the applicability of the Granger causality analysis in our study.

Given two time-series $\{x_i\}$ and $\{y_i\}$, where $i = 1, 2, ..., M$, instantaneous phases were first extracted using the Hilbert transform. Let $\{x_i^p\}$ and $\{y_i^p\}$, where $i = 1, 2, ..., M$, denote the corresponding phase time-series. If the uncertainty of the target signal $\{y_i^p\}$ at delay τ is quantified using Shannon entropy, then the PTE from driver signal $\{x_i^p\}$ to target signal $\{y_i^p\}$ can be given by

$$PTE_{x \to y} = \sum_i p\left(y_{i+\tau}^p, y_i^p, x_i^p\right) \log\left(\frac{p\left(y_{i+\tau}^p \mid y_i^p, x_i^p\right)}{p\left(y_{i+\tau}^p \mid y_i^p\right)}\right), \quad \text{(i)}$$

where the probabilities can be calculated by building histograms of occurrences of singles, pairs, or triplets of instantaneous phase estimates from the phase time-series (Hillebrand et al., 2016). For our analysis, the number of bins in the histograms was set as $3.49 \times STD \times M^{-1/3}$ and delay τ was set as $2M / M_{\pm}$, where STD is average standard deviation of the phase time-series $\{x_i^p\}$ and $\{y_i^p\}$ and $M_{\pm}$ is the number of times the phase changes sign across time and channels (Hillebrand et al., 2016). PTE has been shown to be robust against the choice of the delay τ and the number of bins for forming the histograms (Hillebrand et al., 2016).

Statistical analysis

Statistical analysis was conducted using mixed effects analysis with the lmerTest package (Kuznetsova, Brockhoff, & Christensen, 2017) implemented in R software (version 4.0.2, R Foundation for Statistical Computing). Because PTE data were not normally distributed, we used BestNormalize (Peterson & Cavanaugh, 2018) which contains a suite of transformation-estimating functions that can be used to optimally normalize data. The resulting normally distributed data were subjected to mixed effects analysis with the following model: *PTE ~ Condition + (1|Subject)*, where *Condition* models the fixed effects (condition differences) and (1|*Subject*) models the random repeated measurements within the same participant. Analysis of variance (ANOVA) was used to test the significance of findings with FDR-corrections for multiple comparisons ($p<0.05$). Similar mixed effects statistical analysis procedures were used for comparison of high-gamma power across task conditions, where the mixed effects analysis was run on each of the 0.2s windows.

Finally, we conducted surrogate analysis to test the significance of the estimated PTE values (Hillebrand et al., 2016). The estimated phases from the Hilbert transform for electrodes from a given pair of brain areas were time-shuffled so that the predictability of one time-series from another is destroyed, and PTE analysis was repeated on this shuffled data to build a distribution of surrogate PTE values against which the observed PTE was tested ($p<0.05$).

Bayesian replication analysis

We used replication Bayes factor (Ly et al., 2019; Verhagen & Wagenmakers, 2014) analysis to estimate the degree of replicability for the direction of information flow for each frequency and task condition and across task domains. Analysis was implemented in R software using the BayesFactor package (Rouder, Speckman, Sun, Morey, & Iverson, 2009). Because PTE data were not normally distributed, as previously, we used BestNormalize (Peterson & Cavanaugh, 2018) to optimally normalize data. We calculated the replication Bayes factor for pairwise task domains. We compared the Bayes factor of the joint model *PTE(task1+task2) ~ Condition + (1|Subject)* with the Bayes factor (BF) of individual model as *PTE(task1) ~ Condition + (1|Subject)*, where *task1* denotes the verbal free recall (original) task and *task2* denotes the categorized verbal free recall, or water maze spatial navigation (replication) conditions. We calculated the ratio *BF(task1+task2)/BF(task1)*, which was used to quantify the degree of replicability. We determined whether the degree of replicability was higher than 3 as Bayes factor of at least 3 indicates evidence for replicability (Jeffreys, 1998). A Bayes factor of at least 100 is considered as "*decisive*" for degree of replication (Jeffreys, 1998).

Figure Captions

Figure 1. Task design of the encoding and recall periods of the memory experiments, and iEEG recording sites in the HIPP, with the lateral and medial nodes of the parietal cortex. (a) Experiment 1, Verbal free recall (VFR): (i) Task design of memory encoding and recall periods of the verbal free recall experiment (see **Methods** for details). Participants were first presented with a list of words in the encoding block and asked to recall as many as possible from the original list after a short delay. **(ii)** Electrode locations for HIPP with lateral nodes (top panel) and HIPP with medial nodes (bottom panel), in the verbal free recall experiment. **(b) Experiment 2, Categorized verbal free recall (CATVFR): (i)** Task design of memory encoding and recall periods of the categorized verbal free recall experiment (see **Methods** for details). Participants were presented with a list of words with consecutive pairs of words from a specific category (for example, JEANS-COAT, GRAPE-PEACH, etc.) in the encoding block and subsequently asked to recall as many as possible from the original list after a short delay. **(ii)** Electrode locations for HIPP with lateral nodes (top panel) and HIPP with medial nodes (bottom panel), in the categorized verbal free recall experiment. **(c) Experiment 3, Water maze spatial memory (WMSM): (i)** Task design of memory encoding and recall periods of the water maze spatial memory experiment (see **Methods** for details). Participants were shown objects in various locations during the encoding period and asked to retrieve the location of the objects during the recall period. Modified from Jacobs et. al. (2018) with permission. **(ii)** Electrode locations for HIPP with lateral nodes (top panel) and HIPP with medial nodes (bottom panel), in the water maze spatial memory experiment. HIPP: hippocampus, dPPC: dorsal posterior parietal cortex, vPPC: ventral posterior parietal cortex, PCC: posterior cingulate cortex, Pr: precuneus.

Figure 2. Directed information flow between hippocampus and dorsal and ventral subdivisions of the posterior parietal cortex (dPPC and vPPC) and PCC/precuneus in broadband (0.5-160 Hz), measured using phase transfer entropy (PTE). (a) Experiment 1, VFR: The hippocampus showed higher causal influences on the dPPC (HIPP → dPPC) (n=208), vPPC (HIPP → vPPC) (n=72), and PCC/precuneus (HIPP → PCC/Pr) (n=53) during both memory encoding and recall, compared to the reverse direction (dPPC → HIPP, vPPC → HIPP, and PCC/Pr → HIPP respectively). **(b) Experiment 2, CATVFR:** The hippocampus showed higher causal directed information flow to the dPPC (HIPP → dPPC) (n=105), vPPC (HIPP → vPPC) (n=50), and PCC/precuneus (HIPP → PCC/Pr) (n=31) during both memory encoding and recall, compared to the reverse direction (dPPC → HIPP, vPPC → HIPP, and PCC/Pr → HIPP respectively). **(c) Experiment 3, WMSM:** The hippocampus also showed higher causal influences on the dPPC (HIPP → dPPC) (n=104), vPPC (HIPP → vPPC) (n=19), and PCC/precuneus (HIPP → PCC/Pr) (n=31) during both memory encoding and recall, compared to the reverse direction (dPPC → HIPP, vPPC → HIPP, and PCC/Pr → HIPP respectively). *** $p < 0.001$, ** $p < 0.01$ (Linear mixed effects ANOVA, FDR-corrected).

Figure 3. Directed information flow between hippocampus and dorsal and ventral subdivisions of the posterior parietal cortex (dPPC and vPPC) and PCC/precuneus in delta-theta band (0.5-8 Hz). (a) Experiment 1, VFR: The hippocampus showed higher causal influences on the dPPC (HIPP → dPPC) (n=208), vPPC (HIPP → vPPC) (n=72), and PCC/precuneus (HIPP → PCC/Pr) (n=53) during both memory encoding and recall, compared to the reverse direction (dPPC → HIPP, vPPC → HIPP, and PCC/Pr → HIPP respectively). **(b) Experiment 2, CATVFR:** The hippocampus showed higher causal directed information flow to

the dPPC (HIPP → dPPC) (n=105), vPPC (HIPP → vPPC) (n=50), and PCC/precuneus (HIPP → PCC/Pr) (n=31) during both memory encoding and recall, compared to the reverse direction (dPPC → HIPP, vPPC → HIPP, and PCC/Pr → HIPP respectively). **(c) Experiment 3, WMSM:** The hippocampus also showed higher causal influences on the dPPC (HIPP → dPPC) (n=104), vPPC (HIPP → vPPC) (n=19), and PCC/precuneus (HIPP → PCC/Pr) (n=31) during both memory encoding and recall, compared to the reverse direction (dPPC → HIPP, vPPC → HIPP, and PCC/Pr → HIPP respectively). *** $p < 0.001$ (Linear mixed effects ANOVA, FDR-corrected).

Figure 4. Directed information flow between hippocampus and dorsal and ventral subdivisions of the posterior parietal cortex (dPPC and vPPC) and PCC/precuneus in beta band (12-30 Hz). (a) Experiment 1, VFR: dPPC (dPPC → HIPP) (n=208), vPPC (vPPC → HIPP) (n=72), and PCC/precuneus (PCC/Pr → HIPP) (n=53) showed higher causal influences on the hippocampus during both memory encoding and recall, compared to the reverse direction (HIPP → dPPC, HIPP → vPPC, and HIPP → PCC/Pr respectively). **(b) Experiment 2, CATVFR:** dPPC (dPPC → HIPP) (n=105), vPPC (vPPC → HIPP) (n=50), and PCC/precuneus (PCC/Pr → HIPP) (n=31) showed higher causal influences on the hippocampus during both memory encoding and recall, compared to the reverse direction (HIPP → dPPC, HIPP → vPPC, and HIPP → PCC/Pr respectively). **(c) Experiment 3, WMSM:** dPPC (dPPC → HIPP) (n=104), vPPC (vPPC → HIPP) (n=19), and PCC/precuneus (PCC/Pr → HIPP) (n=31) also showed higher causal influences on the hippocampus during both memory encoding and recall, compared to the reverse direction (HIPP → dPPC, HIPP → vPPC, and HIPP → PCC/Pr respectively). *** $p < 0.001$, ** $p < 0.01$, * $p < 0.05$ (Linear mixed effects ANOVA, FDR-corrected).

Figure 5. iEEG evoked response, quantified using high-gamma power (HGP), for HIPP (red) and dorsal PPC (blue), ventral PPC (cyan), and PCC/precuneus (orange) during (a) VFR, (b) CATVFR, and (c) WMSM experiments. (a) Experiment 1, VFR: Evoked response during encoding and recall in the verbal free recall task, quantified using HGP (see **Methods**). **(b) Experiment 2, CATVFR:** Evoked response during encoding and recall in the categorized verbal free recall task. **(c) Experiment 3, WMSM:** Evoked response during encoding and recall in the water maze spatial memory task. Horizontal green lines denote *ps* < 0.05.

Figure 6. Schematic illustration of key findings related to the intracranial electrophysiology of directed information flow between the hippocampus and the lateral and medial parietal cortex in human episodic memory. Despite variable patterns of local activation and suppression of the lateral and medial parietal cortex compared to the hippocampus during memory encoding and recall, we found **(a)** stronger causal influence (denoted by green arrows, thickness of arrows denotes degree of replicability across experiments, see **Table 1**) by the hippocampus on the lateral and medial parietal cortex than the reverse, in broadband, across all three memory experiments, and during both encoding and recall periods. Frequency specific analysis revealed **(b)** stronger causal influence by the hippocampus on the lateral and medial parietal cortex than the reverse, in the delta-theta band, across all three memory experiments, and during both encoding and recall periods. This analysis also revealed **(c)** stronger causal influence by the lateral and medial parietal cortex on the hippocampus than the reverse, in the beta band, across all three memory experiments, and during both encoding and recall periods. These

findings suggest robust and replicable frequency-dependent feedforward and feedback signaling between the hippocampus and the posterior parietal cortex in human episodic memory.

Tables

Table 1. Replicability of findings of causal interactions of the hippocampus with dPPC, vPPC, and PCC/Pr across verbal free recall, categorized verbal free recall, and water maze spatial memory domains. (a) Memory Encoding and (b) Memory Recall. The verbal free recall (VFR) task was considered the original dataset and the categorized verbal free recall (CATVFR) and water maze spatial memory (WMSM) tasks were considered replication datasets and Bayes factor (BF) for replication was calculated for pairwise tasks (verbal free recall vs. T, where T can be categorized verbal free recall, or water maze spatial memory task). dPPC: dorsal posterior parietal cortex, vPPC: ventral posterior parietal cortex, PCC: posterior cingulate cortex, Pr: precuneus.

(a) Memory Encoding

(i) Broadband

Finding	**Bayes Factor for VFR-CATVFR replication**	**Bayes Factor for VFR-WMSN replication**
HIPP → dPPC > dPPC → HIPP	7.61e+35	3.84e+16
HIPP → vPPC > vPPC → HIPP	5.91e+0	3.84e+16
HIPP → PCC/Pr > PCC/Pr → HIPP	1.04e+4	4.67e+0

(ii) Delta-theta

HIPP → dPPC > dPPC → HIPP	1.58e+4	8.73e+33
HIPP → vPPC > vPPC → HIPP	1.44e+5	1.85e+2
HIPP → PCC/Pr > PCC/Pr → HIPP	9.46e+8	1.61e+16

(iii) Beta

HIPP → dPPC < dPPC → HIPP	1.47e+30	5.05e+34
HIPP → vPPC < vPPC → HIPP	2.53e+16	2.36e+7
HIPP → PCC/Pr < PCC/Pr → HIPP	6.64e+5	5.15e-1

(b) Memory Recall

(i) Broadband

Finding	**Bayes Factor for VFR-CATVFR replication**	**Bayes Factor for VFR-WMSN replication**
HIPP → dPPC > dPPC → HIPP	6.78e+36	1.42e+14
HIPP → vPPC > vPPC → HIPP	1.54e+1	9.61e+0
HIPP → PCC/Pr > PCC/Pr → HIPP	2.77e+4	6.13e+1

(ii) Delta-theta

HIPP → dPPC > dPPC → HIPP	1.38e+12	1.55e+31
HIPP → vPPC > vPPC → HIPP	4.29e+8	9.88e+1
HIPP → PCC/Pr > PCC/Pr → HIPP	9.55e+8	7.31e+12

(iii) Beta

HIPP → dPPC < dPPC → HIPP	3.56e+13	6.65e+28
HIPP → vPPC < vPPC → HIPP	7.32e+11	1.99e+8
HIPP → PCC/Pr < PCC/Pr → HIPP	8.19e+1	3.88e+1

References

Andersen, R. A., Essick, G. K., & Siegel, R. M. (1985). Encoding of spatial location by posterior parietal neurons. *Science, 230*(4724), 456-458. doi:10.1126/science.4048942

Andrews-Hanna, J. R. (2012). The brain's default network and its adaptive role in internal mentation. *Neuroscientist, 18*(3), 251-270. doi:10.1177/1073858411403316

Auger, S. D., & Maguire, E. A. (2013). Assessing the mechanism of response in the retrosplenial cortex of good and poor navigators. *Cortex, 49*(10), 2904-2913. doi:10.1016/j.cortex.2013.08.002

Badre, D., Poldrack, R. A., Paré-Blagoev, E. J., Insler, R. Z., & Wagner, A. D. (2005). Dissociable controlled retrieval and generalized selection mechanisms in ventrolateral prefrontal cortex. *Neuron, 47*(6), 907-918. doi:10.1016/j.neuron.2005.07.023

Badre, D., & Wagner, A. D. (2007). Left ventrolateral prefrontal cortex and the cognitive control of memory. *Neuropsychologia, 45*(13), 2883-2901. doi:10.1016/j.neuropsychologia.2007.06.015

Barnett, L., & Seth, A. K. (2014). The MVGC multivariate Granger causality toolbox: A new approach to Granger-causal inference. *Journal of Neuroscience Methods, 223*, 50-68. doi:10.1016/j.jneumeth.2013.10.018

Barrow, C. J., & Latto, R. (1996). The role of inferior parietal cortex and fornix in route following and topographic orientation in cynomolgus monkeys. *Behav Brain Res, 75*(1-2), 99-112. doi:10.1016/0166-4328(96)00177-5

Bastos, A. M., Vezoli, J., Bosman, C. A., Schoffelen, J. M., Oostenveld, R., Dowdall, J. R., . . . Fries, P. (2015). Visual areas exert feedforward and feedback influences through distinct frequency channels. *Neuron, 85*(2), 390-401. doi:10.1016/j.neuron.2014.12.018

Bellana, B., Ladyka-Wojcik, N., Lahan, S., Moscovitch, M., & Grady, C. L. (2023). Recollection and prior knowledge recruit the left angular gyrus during recognition. *Brain Struct Funct, 228*(1), 197-217. doi:10.1007/s00429-022-02597-5

Benoit, R. G., & Schacter, D. L. (2015). Specifying the core network supporting episodic simulation and episodic memory by activation likelihood estimation. *Neuropsychologia, 75*, 450-457. doi:10.1016/j.neuropsychologia.2015.06.034

Bohbot, V. D., Kalina, M., Stepankova, K., Spackova, N., Petrides, M., & Nadel, L. (1998). Spatial memory deficits in patients with lesions to the right hippocampus and to the right parahippocampal cortex. *Neuropsychologia, 36*(11), 1217-1238. doi:10.1016/s0028-3932(97)00161-9

Bressler, S. L., & Menon, V. (2010). Large-scale brain networks in cognition: emerging methods and principles. *Trends in Cognitive Sciences, 14*(6), 277-290. doi:10.1016/j.tics.2010.04.004

Brodt, S., Gais, S., Beck, J., Erb, M., Scheffler, K., & Schönauer, M. (2018). Fast track to the neocortex: A memory engram in the posterior parietal cortex. *Science, 362*(6418), 1045-1048. doi:10.1126/science.aau2528

Brodt, S., Pöhlchen, D., Flanagin, V. L., Glasauer, S., Gais, S., & Schönauer, M. (2016). Rapid and independent memory formation in the parietal cortex. *Proc Natl Acad Sci U S A, 113*(46), 13251-13256. doi:10.1073/pnas.1605719113

Brovelli, A., Ding, M., Ledberg, A., Chen, Y., Nakamura, R., & Bressler, S. L. (2004). Beta oscillations in a large-scale sensorimotor cortical network: directional influences revealed

by Granger causality. *Proc Natl Acad Sci U S A, 101*(26), 9849-9854. doi:10.1073/pnas.0308538101
Buckner, R. L., Andrews-Hanna, J. R., & Schacter, D. L. (2008). The brain's default network: anatomy, function, and relevance to disease. *Ann N Y Acad Sci, 1124*, 1-38. doi:10.1196/annals.1440.011
Buckner, R. L., Koutstaal, W., Schacter, D. L., Dale, A. M., Rotte, M., & Rosen, B. R. (1998). Functional-anatomic study of episodic retrieval. II. Selective averaging of event-related fMRI trials to test the retrieval success hypothesis. *Neuroimage, 7*(3), 163-175. doi:10.1006/nimg.1998.0328
Burgess, N., Maguire, E. A., & O'Keefe, J. (2002). The human hippocampus and spatial and episodic memory. *Neuron, 35*(4), 625-641. doi:10.1016/s0896-6273(02)00830-9
Burke, J. F., Sharan, A. D., Sperling, M. R., Ramayya, A. G., Evans, J. J., Healey, M. K., . . . Kahana, M. J. (2014). Theta and high-frequency activity mark spontaneous recall of episodic memories. *J Neurosci, 34*(34), 11355-11365. doi:10.1523/jneurosci.2654-13.2014
Burke, J. F., Zaghloul, K. A., Jacobs, J., Williams, R. B., Sperling, M. R., Sharan, A. D., & Kahana, M. J. (2013). Synchronous and asynchronous theta and gamma activity during episodic memory formation. *J Neurosci, 33*(1), 292-304. doi:10.1523/jneurosci.2057-12.2013
Cabeza, R. (2008). Role of parietal regions in episodic memory retrieval: the dual attentional processes hypothesis. *Neuropsychologia, 46*(7), 1813-1827. doi:10.1016/j.neuropsychologia.2008.03.019
Cabeza, R., Ciaramelli, E., & Moscovitch, M. (2012). Cognitive contributions of the ventral parietal cortex: an integrative theoretical account. *Trends Cogn Sci, 16*(6), 338-352. doi:10.1016/j.tics.2012.04.008
Cabeza, R., Ciaramelli, E., Olson, I. R., & Moscovitch, M. (2008). The parietal cortex and episodic memory: an attentional account. *Nat Rev Neurosci, 9*(8), 613-625. doi:10.1038/nrn2459
Cabeza, R., Mazuz, Y. S., Stokes, J., Kragel, J. E., Woldorff, M. G., Ciaramelli, E., . . . Moscovitch, M. (2011). Overlapping parietal activity in memory and perception: evidence for the attention to memory model. *J Cogn Neurosci, 23*(11), 3209-3217. doi:10.1162/jocn_a_00065
Canales-Johnson, A., Teixeira Borges, A. F., Komatsu, M., Fujii, N., Fahrenfort, J. J., Miller, K. J., & Noreika, V. (2021). Broadband Dynamics Rather than Frequency-Specific Rhythms Underlie Prediction Error in the Primate Auditory Cortex. *J Neurosci, 41*(45), 9374-9391. doi:10.1523/jneurosci.0367-21.2021
Canolty, R. T., Edwards, E., Dalal, S. S., Soltani, M., Nagarajan, S. S., Kirsch, H. E., . . . Knight, R. T. (2006). High gamma power is phase-locked to theta oscillations in human neocortex. *Science, 313*(5793), 1626-1628. doi:10.1126/science.1128115
Canolty, R. T., & Knight, R. T. (2010). The functional role of cross-frequency coupling. *Trends Cogn Sci, 14*(11), 506-515. doi:10.1016/j.tics.2010.09.001
Chen, L. L., Lin, L. H., Green, E. J., Barnes, C. A., & McNaughton, B. L. (1994). Head-direction cells in the rat posterior cortex. I. Anatomical distribution and behavioral modulation. *Exp Brain Res, 101*(1), 8-23. doi:10.1007/bf00243212
Ciaramelli, E., Burianová, H., Vallesi, A., Cabeza, R., & Moscovitch, M. (2020). Functional Interplay Between Posterior Parietal Cortex and Hippocampus During Detection of

Memory Targets and Non-targets. *Front Neurosci, 14*, 563768. doi:10.3389/fnins.2020.563768
Ciaramelli, E., Grady, C. L., & Moscovitch, M. (2008). Top-down and bottom-up attention to memory: a hypothesis (AtoM) on the role of the posterior parietal cortex in memory retrieval. *Neuropsychologia, 46*(7), 1828-1851. doi:10.1016/j.neuropsychologia.2008.03.022
Clower, D. M., West, R. A., Lynch, J. C., & Strick, P. L. (2001). The inferior parietal lobule is the target of output from the superior colliculus, hippocampus, and cerebellum. *J Neurosci, 21*(16), 6283-6291. doi:10.1523/jneurosci.21-16-06283.2001
Corbetta, M. (1998). Frontoparietal cortical networks for directing attention and the eye to visual locations: identical, independent, or overlapping neural systems? *Proc Natl Acad Sci U S A, 95*(3), 831-838. doi:10.1073/pnas.95.3.831
Crone, N. E., Boatman, D., Gordon, B., & Hao, L. (2001). Induced electrocorticographic gamma activity during auditory perception. Brazier Award-winning article, 2001. *Clin Neurophysiol, 112*(4), 565-582. doi:10.1016/s1388-2457(00)00545-9
Crossman, M., Bartl, G., Soerum, R., & Sandrini, M. (2019). Effects of transcranial direct current stimulation over the posterior parietal cortex on episodic memory reconsolidation. *Cortex, 121*, 78-88. doi:10.1016/j.cortex.2019.08.009
Crowe, D. A., Chafee, M. V., Averbeck, B. B., & Georgopoulos, A. P. (2004). Neural activity in primate parietal area 7a related to spatial analysis of visual mazes. *Cereb Cortex, 14*(1), 23-34. doi:10.1093/cercor/bhg088
Curtis, C. E. (2006). Prefrontal and parietal contributions to spatial working memory. *Neuroscience, 139*(1), 173-180. doi:10.1016/j.neuroscience.2005.04.070
Daitch, A. L., & Parvizi, J. (2018). Spatial and temporal heterogeneity of neural responses in human posteromedial cortex. *Proc Natl Acad Sci U S A, 115*(18), 4785-4790. doi:10.1073/pnas.1721714115
Das, A., de Los Angeles, C., & Menon, V. (2022). Electrophysiological foundations of the human default-mode network revealed by intracranial-EEG recordings during resting-state and cognition. *Neuroimage, 250*, 118927. doi:10.1016/j.neuroimage.2022.118927
Das, A., & Menon, V. (2020). Spatiotemporal Integrity and Spontaneous Nonlinear Dynamic Properties of the Salience Network Revealed by Human Intracranial Electrophysiology: A Multicohort Replication. *Cereb Cortex, 30*(10), 5309-5321. doi:10.1093/cercor/bhaa111
Das, A., & Menon, V. (2021). Asymmetric Frequency-Specific Feedforward and Feedback Information Flow between Hippocampus and Prefrontal Cortex during Verbal Memory Encoding and Recall. *J Neurosci, 41*(40), 8427-8440. doi:10.1523/jneurosci.0802-21.2021
Das, A., & Menon, V. (2022a). Causal dynamics and information flow in parietal-temporal-hippocampal circuits during mental arithmetic revealed by high-temporal resolution human intracranial EEG. *Cortex, 147*, 24-40. doi:10.1016/j.cortex.2021.11.012
Das, A., & Menon, V. (2022b). Replicable patterns of causal information flow between hippocampus and prefrontal cortex during spatial navigation and spatial-verbal memory formation. *Cereb Cortex, 32*(23), 5343-5361. doi:10.1093/cercor/bhac018
Das, A., & Menon, V. (2023). Concurrent- and after-effects of medial temporal lobe stimulation on directed information flow to and from prefrontal and parietal cortices during memory formation. *J Neurosci, 43*(17), 3159-3175. doi:10.1523/jneurosci.1728-22.2023

Daselaar, S. M., Prince, S. E., Dennis, N. A., Hayes, S. M., Kim, H., & Cabeza, R. (2009). Posterior midline and ventral parietal activity is associated with retrieval success and encoding failure. *Front Hum Neurosci, 3*, 13. doi:10.3389/neuro.09.013.2009

Dickerson, B. C., & Eichenbaum, H. (2010). The episodic memory system: neurocircuitry and disorders. *Neuropsychopharmacology, 35*(1), 86-104. doi:10.1038/npp.2009.126

Donoghue, T., Haller, M., Peterson, E. J., Varma, P., Sebastian, P., Gao, R., . . . Voytek, B. (2020). Parameterizing neural power spectra into periodic and aperiodic components. *Nat Neurosci, 23*(12), 1655-1665. doi:10.1038/s41593-020-00744-x

Edwards, E., Soltani, M., Deouell, L. Y., Berger, M. S., & Knight, R. T. (2005). High gamma activity in response to deviant auditory stimuli recorded directly from human cortex. *J Neurophysiol, 94*(6), 4269-4280. doi:10.1152/jn.00324.2005

Eichenbaum, H. (2017). Prefrontal-hippocampal interactions in episodic memory. *Nat Rev Neurosci, 18*(9), 547-558. doi:10.1038/nrn.2017.74

Ekstrom, A. D., Caplan, J. B., Ho, E., Shattuck, K., Fried, I., & Kahana, M. J. (2005). Human hippocampal theta activity during virtual navigation. *Hippocampus, 15*(7), 881-889. doi:10.1002/hipo.20109

Ekstrom, A. D., & Hill, P. F. (2023). Spatial navigation and memory: A review of the similarities and differences relevant to brain models and age. *Neuron, 111*(7), 1037-1049. doi:10.1016/j.neuron.2023.03.001

Ekstrom, A. D., & Watrous, A. J. (2014). Multifaceted roles for low-frequency oscillations in bottom-up and top-down processing during navigation and memory. *Neuroimage, 85 Pt 2*, 667-677. doi:10.1016/j.neuroimage.2013.06.049

Engel, A. K., & Fries, P. (2010). Beta-band oscillations--signalling the status quo? *Curr Opin Neurobiol, 20*(2), 156-165. doi:10.1016/j.conb.2010.02.015

Ezzyat, Y., Wanda, P. A., Levy, D. F., Kadel, A., Aka, A., Pedisich, I., . . . Kahana, M. J. (2018). Closed-loop stimulation of temporal cortex rescues functional networks and improves memory. *Nat Commun, 9*(1), 365. doi:10.1038/s41467-017-02753-0

Fan, L., Li, H., Zhuo, J., Zhang, Y., Wang, J., Chen, L., . . . Jiang, T. (2016). The Human Brainnetome Atlas: A New Brain Atlas Based on Connectional Architecture. *Cereb Cortex, 26*(8), 3508-3526. doi:10.1093/cercor/bhw157

Garrison, K. A., Scheinost, D., Worhunsky, P. D., Elwafi, H. M., Thornhill, T. A. t., Thompson, E., . . . Brewer, J. A. (2013). Real-time fMRI links subjective experience with brain activity during focused attention. *Neuroimage, 81*, 110-118. doi:10.1016/j.neuroimage.2013.05.030

Ghaem, O., Mellet, E., Crivello, F., Tzourio, N., Mazoyer, B., Berthoz, A., & Denis, M. (1997). Mental navigation along memorized routes activates the hippocampus, precuneus, and insula. *Neuroreport, 8*(3), 739-744. doi:10.1097/00001756-199702100-00032

Goldring, A. B., & Krubitzer, L. A. (2020). Evolution of parietal cortex in mammals: from manipulation to tool use. In J. H. Kaas (Ed.), *Evolutionary Neuroscience* (pp. 627-656): Academic Press.

Gonzalez, A., Hutchinson, J. B., Uncapher, M. R., Chen, J., LaRocque, K. F., Foster, B. L., . . . Wagner, A. D. (2015). Electrocorticography reveals the temporal dynamics of posterior parietal cortical activity during recognition memory decisions. *Proc Natl Acad Sci U S A, 112*(35), 11066-11071. doi:10.1073/pnas.1510749112

Goodrich-Hunsaker, N. J., Hunsaker, M. R., & Kesner, R. P. (2005). Dissociating the role of the parietal cortex and dorsal hippocampus for spatial information processing. *Behav Neurosci, 119*(5), 1307-1315. doi:10.1037/0735-7044.119.5.1307

Goyal, A., Miller, J., Watrous, A. J., Lee, S. A., Coffey, T., Sperling, M. R., . . . Jacobs, J. (2018). Electrical Stimulation in Hippocampus and Entorhinal Cortex Impairs Spatial and Temporal Memory. *J Neurosci, 38*(19), 4471-4481. doi:10.1523/jneurosci.3049-17.2018

Greicius, M. D., Krasnow, B., Reiss, A. L., & Menon, V. (2003). Functional connectivity in the resting brain: A network analysis of the default mode hypothesis. *Proceedings of the National Academy of Sciences, 100*(1), 253-258. doi:10.1073/pnas.0135058100

Grön, G., Wunderlich, A. P., Spitzer, M., Tomczak, R., & Riepe, M. W. (2000). Brain activation during human navigation: gender-different neural networks as substrate of performance. *Nat Neurosci, 3*(4), 404-408. doi:10.1038/73980

Gurd, J. M., Amunts, K., Weiss, P. H., Zafiris, O., Zilles, K., Marshall, J. C., & Fink, G. R. (2002). Posterior parietal cortex is implicated in continuous switching between verbal fluency tasks: an fMRI study with clinical implications. *Brain, 125*(Pt 5), 1024-1038. doi:10.1093/brain/awf093

Hillebrand, A., Tewarie, P., van Dellen, E., Yu, M., Carbo, E. W., Douw, L., . . . Stam, C. J. (2016). Direction of information flow in large-scale resting-state networks is frequency-dependent. *Proc Natl Acad Sci U S A, 113*(14), 3867-3872. doi:10.1073/pnas.1515657113

Husain, M., & Nachev, P. (2007). Space and the parietal cortex. *Trends Cogn Sci, 11*(1), 30-36. doi:10.1016/j.tics.2006.10.011

Hutchinson, J. B., Uncapher, M. R., & Wagner, A. D. (2009). Posterior parietal cortex and episodic retrieval: convergent and divergent effects of attention and memory. *Learn Mem, 16*(6), 343-356. doi:10.1101/lm.919109

Hutchison, R. M., Hashemi, N., Gati, J. S., Menon, R. S., & Everling, S. (2015). Electrophysiological signatures of spontaneous BOLD fluctuations in macaque prefrontal cortex. *Neuroimage, 113*, 257-267. doi:10.1016/j.neuroimage.2015.03.062

Iglói, K., Doeller, C. F., Berthoz, A., Rondi-Reig, L., & Burgess, N. (2010). Lateralized human hippocampal activity predicts navigation based on sequence or place memory. *Proc Natl Acad Sci U S A, 107*(32), 14466-14471. doi:10.1073/pnas.1004243107

Insausti, R., & Muñoz, M. (2001). Cortical projections of the non-entorhinal hippocampal formation in the cynomolgus monkey (Macaca fascicularis). *Eur J Neurosci, 14*(3), 435-451. doi:10.1046/j.0953-816x.2001.01662.x

Jacobs, J., Miller, J., Lee, S. A., Coffey, T., Watrous, A. J., Sperling, M. R., . . . Rizzuto, D. S. (2016). Direct Electrical Stimulation of the Human Entorhinal Region and Hippocampus Impairs Memory. *Neuron, 92*(5), 983-990. doi:10.1016/j.neuron.2016.10.062

Jeffreys, H. (1998). *The Theory of Probability* (3rd ed.). Oxford, England: Oxford University Press.

Jonker, T. R., Dimsdale-Zucker, H., Ritchey, M., Clarke, A., & Ranganath, C. (2018). Neural reactivation in parietal cortex enhances memory for episodically linked information. *Proc Natl Acad Sci U S A, 115*(43), 11084-11089. doi:10.1073/pnas.1800006115

Kaplan, R., Horner, A. J., Bandettini, P. A., Doeller, C. F., & Burgess, N. (2014). Human hippocampal processing of environmental novelty during spatial navigation. *Hippocampus, 24*(7), 740-750. doi:10.1002/hipo.22264

Kayser, C., Montemurro, M. A., Logothetis, N. K., & Panzeri, S. (2009). Spike-phase coding boosts and stabilizes information carried by spatial and temporal spike patterns. *Neuron, 61*(4), 597-608. doi:10.1016/j.neuron.2009.01.008

Konishi, S., Wheeler, M. E., Donaldson, D. I., & Buckner, R. L. (2000). Neural correlates of episodic retrieval success. *Neuroimage, 12*(3), 276-286. doi:10.1006/nimg.2000.0614

Korkki, S. M., Richter, F. R., & Simons, J. S. (2021). Hippocampal-Cortical Encoding Activity Predicts the Precision of Episodic Memory. *J Cogn Neurosci, 33*(11), 2328-2341. doi:10.1162/jocn_a_01770

Kuznetsova, A., Brockhoff, P. B., & Christensen, R. H. B. (2017). lmerTest Package: Tests in Linear Mixed Effects Models. *Journal of Statistical Software, 82*(13), 1-26.

Kwon, H., Kronemer, S. I., Christison-Lagay, K. L., Khalaf, A., Li, J., Ding, J. Z., . . . Blumenfeld, H. (2021). Early cortical signals in visual stimulus detection. *Neuroimage, 244*, 118608. doi:10.1016/j.neuroimage.2021.118608

Lachaux, J. P., George, N., Tallon-Baudry, C., Martinerie, J., Hugueville, L., Minotti, L., . . . Renault, B. (2005). The many faces of the gamma band response to complex visual stimuli. *Neuroimage, 25*(2), 491-501. doi:10.1016/j.neuroimage.2004.11.052

Lachaux, J. P., Rodriguez, E., Martinerie, J., & Varela, F. J. (1999). Measuring phase synchrony in brain signals. *Hum Brain Mapp, 8*(4), 194-208. doi:10.1002/(sici)1097-0193(1999)8:4<194::aid-hbm4>3.0.co;2-c

Lakatos, P., Gross, J., & Thut, G. (2019). A New Unifying Account of the Roles of Neuronal Entrainment. *Curr Biol, 29*(18), R890-r905. doi:10.1016/j.cub.2019.07.075

Lee, S. A., Miller, J. F., Watrous, A. J., Sperling, M. R., Sharan, A., Worrell, G. A., . . . Jacobs, J. (2018). Electrophysiological Signatures of Spatial Boundaries in the Human Subiculum. *J Neurosci, 38*(13), 3265-3272. doi:10.1523/jneurosci.3216-17.2018

Leech, R., & Sharp, D. J. (2014). The role of the posterior cingulate cortex in cognition and disease. *Brain, 137*(Pt 1), 12-32. doi:10.1093/brain/awt162

Leopold, D. A., Murayama, Y., & Logothetis, N. K. (2003). Very slow activity fluctuations in monkey visual cortex: implications for functional brain imaging. *Cereb Cortex, 13*(4), 422-433. doi:10.1093/cercor/13.4.422

Lobier, M., Siebenhühner, F., Palva, S., & Matias, P. J. (2014). Phase transfer entropy: A novel phase-based measure for directed connectivity in networks coupled by oscillatory interactions. *Neuroimage, 85*, 853-872. doi:10.1016/j.neuroimage.2013.08.056

Long, N. M., Burke, J. F., & Kahana, M. J. (2014). Subsequent memory effect in intracranial and scalp EEG. *Neuroimage, 84*, 488-494. doi:10.1016/j.neuroimage.2013.08.052

Lopour, B. A., Tavassoli, A., Fried, I., & Ringach, D. L. (2013). Coding of information in the phase of local field potentials within human medial temporal lobe. *Neuron, 79*(3), 594-606. doi:10.1016/j.neuron.2013.06.001

Ly, A., Etz, A., Marsman, M., & Wagenmakers, E. J. (2019). Replication Bayes factors from evidence updating. *Behav Res Methods, 51*(6), 2498-2508. doi:10.3758/s13428-018-1092-x

Maguire, E. A., Burgess, N., Donnett, J. G., Frackowiak, R. S., Frith, C. D., & O'Keefe, J. (1998). Knowing where and getting there: a human navigation network. *Science, 280*(5365), 921-924. doi:10.1126/science.280.5365.921

Maguire, E. A., Burgess, N., & O'Keefe, J. (1999). Human spatial navigation: cognitive maps, sexual dimorphism, and neural substrates. *Curr Opin Neurobiol, 9*(2), 171-177. doi:10.1016/s0959-4388(99)80023-3

Maguire, E. A., Burke, T., Phillips, J., & Staunton, H. (1996). Topographical disorientation following unilateral temporal lobe lesions in humans. *Neuropsychologia, 34*(10), 993-1001. doi:10.1016/0028-3932(96)00022-x

Maguire, E. A., Gadian, D. G., Johnsrude, I. S., Good, C. D., Ashburner, J., Frackowiak, R. S., & Frith, C. D. (2000). Navigation-related structural change in the hippocampi of taxi drivers. *Proc Natl Acad Sci U S A, 97*(8), 4398-4403. doi:10.1073/pnas.070039597

Mainy, N., Kahane, P., Minotti, L., Hoffmann, D., Bertrand, O., & Lachaux, J. P. (2007). Neural correlates of consolidation in working memory. *Hum Brain Mapp, 28*(3), 183-193. doi:10.1002/hbm.20264

Mantini, D., Perrucci, M. G., Del Gratta, C., Romani, G. L., & Corbetta, M. (2007). Electrophysiological signatures of resting state networks in the human brain. *Proc Natl Acad Sci U S A, 104*(32), 13170-13175. doi:10.1073/pnas.0700668104

McNaughton, B. L., Mizumori, S. J., Barnes, C. A., Leonard, B. J., Marquis, M., & Green, E. J. (1994). Cortical representation of motion during unrestrained spatial navigation in the rat. *Cereb Cortex, 4*(1), 27-39. doi:10.1093/cercor/4.1.27

Menon, V. (2023). 20 years of the default mode network: a review and synthesis. *Neuron*.

Menon, V., Freeman, W. J., Cutillo, B. A., Desmond, J. E., Ward, M. F., Bressler, S. L., . . . Gevins, A. S. (1996). Spatio-temporal correlations in human gamma band electrocorticograms. *Electroencephalography and Clinical Neurophysiology, 98*(2), 89-102. doi:10.1016/0013-4694(95)00206-5

Miller, J., Watrous, A. J., Tsitsiklis, M., Lee, S. A., Sheth, S. A., Schevon, C. A., . . . Jacobs, J. (2018). Lateralized hippocampal oscillations underlie distinct aspects of human spatial memory and navigation. *Nat Commun, 9*(1), 2423. doi:10.1038/s41467-018-04847-9

Miller, K. J., Leuthardt, E. C., Schalk, G., Rao, R. P., Anderson, N. R., Moran, D. W., . . . Ojemann, J. G. (2007). Spectral changes in cortical surface potentials during motor movement. *J Neurosci, 27*(9), 2424-2432. doi:10.1523/jneurosci.3886-06.2007

Miyamoto, K., Osada, T., Adachi, Y., Matsui, T., Kimura, H. M., & Miyashita, Y. (2013). Functional differentiation of memory retrieval network in macaque posterior parietal cortex. *Neuron, 77*(4), 787-799. doi:10.1016/j.neuron.2012.12.019

Morris, R. (1984). Developments of a water-maze procedure for studying spatial learning in the rat. *J Neurosci Methods, 11*(1), 47-60. doi:10.1016/0165-0270(84)90007-4

Moscovitch, M., Cabeza, R., Winocur, G., & Nadel, L. (2016). Episodic Memory and Beyond: The Hippocampus and Neocortex in Transformation. *Annu Rev Psychol, 67*, 105-134. doi:10.1146/annurev-psych-113011-143733

Negrón-Oyarzo, I., Espinosa, N., Aguilar-Rivera, M., Fuenzalida, M., Aboitiz, F., & Fuentealba, P. (2018). Coordinated prefrontal-hippocampal activity and navigation strategy-related prefrontal firing during spatial memory formation. *Proc Natl Acad Sci U S A, 115*(27), 7123-7128. doi:10.1073/pnas.1720117115

Neuner, I., Arrubla, J., Werner, C. J., Hitz, K., Boers, F., Kawohl, W., & Shah, N. J. (2014). The default mode network and EEG regional spectral power: a simultaneous fMRI-EEG study. *PLoS One, 9*(2), e88214. doi:10.1371/journal.pone.0088214

Ng, B. S., Logothetis, N. K., & Kayser, C. (2013). EEG phase patterns reflect the selectivity of neural firing. *Cereb Cortex, 23*(2), 389-398. doi:10.1093/cercor/bhs031

Nitz, D. A. (2006). Tracking route progression in the posterior parietal cortex. *Neuron, 49*(5), 747-756. doi:10.1016/j.neuron.2006.01.037

Niu, M., & Palomero-Gallagher, N. (2023). Architecture and connectivity of the human angular gyrus and of its homolog region in the macaque brain. *Brain Struct Funct, 228*(1), 47-61. doi:10.1007/s00429-022-02509-7

Osipova, D., Takashima, A., Oostenveld, R., Fernández, G., Maris, E., & Jensen, O. (2006). Theta and gamma oscillations predict encoding and retrieval of declarative memory. *J Neurosci, 26*(28), 7523-7531. doi:10.1523/jneurosci.1948-06.2006

Paller, K. A., Kutas, M., & McIsaac, H. K. (1995). Monitoring conscious recollection via the electrical activity of the brain. *Psychological Science, 6*(2), 107-111.

Paller, K. A., McCarthy, G., Roessler, E., Allison, T., & Wood, C. C. (1992). Potentials evoked in human and monkey medial temporal lobe during auditory and visual oddball paradigms. *Electroencephalogr Clin Neurophysiol, 84*(3), 269-279. doi:10.1016/0168-5597(92)90008-y

Paller, K. A., McCarthy, G., & Wood, C. C. (1988). ERPs predictive of subsequent recall and recognition performance. *Biol Psychol, 26*(1-3), 269-276. doi:10.1016/0301-0511(88)90023-3

Peterson, R. A., & Cavanaugh, J. E. (2018). Ordered quantile normalization: a semiparametric transformation built for the cross-validation era. *Journal of Applied Statistics, 82*(13-15), 2312–2327.

Pu, Y., Cornwell, B. R., Cheyne, D., & Johnson, B. W. (2017). The functional role of human right hippocampal/parahippocampal theta rhythm in environmental encoding during virtual spatial navigation. *Hum Brain Mapp, 38*(3), 1347-1361. doi:10.1002/hbm.23458

Qasim, S. E., Mohan, U. R., Stein, J. M., & Jacobs, J. (2023). Neuronal activity in the human amygdala and hippocampus enhances emotional memory encoding. *Nat Hum Behav*. doi:10.1038/s41562-022-01502-8

Raccah, O., Daitch, A. L., Kucyi, A., & Parvizi, J. (2018). Direct Cortical Recordings Suggest Temporal Order of Task-Evoked Responses in Human Dorsal Attention and Default Networks. *J Neurosci, 38*(48), 10305-10313. doi:10.1523/jneurosci.0079-18.2018

Raichle, M. E., MacLeod, A. M., Snyder, A. Z., Powers, W. J., Gusnard, D. A., & Shulman, G. L. (2001). A default mode of brain function. *Proc Natl Acad Sci U S A, 98*(2), 676-682. doi:10.1073/pnas.98.2.676

Ray, S., Crone, N. E., Niebur, E., Franaszczuk, P. J., & Hsiao, S. S. (2008). Neural correlates of high-gamma oscillations (60-200 Hz) in macaque local field potentials and their potential implications in electrocorticography. *J Neurosci, 28*(45), 11526-11536. doi:10.1523/jneurosci.2848-08.2008

Rockland, K. S., & Graves, W. W. (2023). The angular gyrus: a special issue on its complex anatomy and function. *Brain Struct Funct, 228*(1), 1-5. doi:10.1007/s00429-022-02596-6

Rockland, K. S., & Van Hoesen, G. W. (1999). Some temporal and parietal cortical connections converge in CA1 of the primate hippocampus. *Cereb Cortex, 9*(3), 232-237. doi:10.1093/cercor/9.3.232

Rogers, J. L., & Kesner, R. P. (2006). Lesions of the dorsal hippocampus or parietal cortex differentially affect spatial information processing. *Behav Neurosci, 120*(4), 852-860. doi:10.1037/0735-7044.120.4.852

Rogers, J. L., & Kesner, R. P. (2007). Hippocampal-parietal cortex interactions: evidence from a disconnection study in the rat. *Behav Brain Res, 179*(1), 19-27. doi:10.1016/j.bbr.2007.01.019

Rolls, E. T. (2018). The storage and recall of memories in the hippocampo-cortical system. *Cell Tissue Res, 373*(3), 577-604. doi:10.1007/s00441-017-2744-3

Rolls, E. T. (2019). The cingulate cortex and limbic systems for action, emotion, and memory. *Handb Clin Neurol, 166*, 23-37. doi:10.1016/b978-0-444-64196-0.00002-9

Rouder, J. N., Speckman, P. L., Sun, D., Morey, R. D., & Iverson, G. (2009). Bayesian t tests for accepting and rejecting the null hypothesis. *Psychon Bull Rev, 16*(2), 225-237. doi:10.3758/pbr.16.2.225

Rubinstein, D. Y., Camarillo-Rodriguez, L., Serruya, M. D., Herweg, N. A., Waldman, Z. J., Wanda, P. A., . . . Sperling, M. R. (2021). Contribution of left supramarginal and angular gyri to episodic memory encoding: An intracranial EEG study. *Neuroimage, 225*, 117514. doi:10.1016/j.neuroimage.2020.117514

Rugg, M. D., Mark, R. E., Walla, P., Schloerscheidt, A. M., Birch, C. S., & Allan, K. (1998). Dissociation of the neural correlates of implicit and explicit memory. *Nature, 392*(6676), 595-598. doi:10.1038/33396

Rugg, M. D., & Vilberg, K. L. (2013). Brain networks underlying episodic memory retrieval. *Curr Opin Neurobiol, 23*(2), 255-260. doi:10.1016/j.conb.2012.11.005

Scholvinck, M. L., Maier, A., Ye, F. Q., Duyn, J. H., & Leopold, D. A. (2010). Neural basis of global resting-state fMRI activity. *Proc Natl Acad Sci U S A, 107*(22), 10238-10243. doi:10.1073/pnas.0913110107

Schultheiss, N. W., Schlecht, M., Jayachandran, M., Brooks, D. R., McGlothan, J. L., Guilarte, T. R., & Allen, T. A. (2020). Awake delta and theta-rhythmic hippocampal network modes during intermittent locomotor behaviors in the rat. *Behav Neurosci*. doi:10.1037/bne0000409

Sederberg, P. B., Schulze-Bonhage, A., Madsen, J. R., Bromfield, E. B., Litt, B., Brandt, A., & Kahana, M. J. (2007). Gamma oscillations distinguish true from false memories. *Psychol Sci, 18*(11), 927-932. doi:10.1111/j.1467-9280.2007.02003.x

Seger, S. E., Kriegel, J. L. S., Lega, B. C., & Ekstrom, A. D. (2023). Memory-related processing is the primary driver of human hippocampal theta oscillations. *Neuron, 111*(19), 3119-3130.e3114. doi:10.1016/j.neuron.2023.06.015

Seghier, M. L. (2013). The angular gyrus: multiple functions and multiple subdivisions. *Neuroscientist, 19*(1), 43-61. doi:10.1177/1073858412440596

Seghier, M. L. (2023). Multiple functions of the angular gyrus at high temporal resolution. *Brain Struct Funct, 228*(1), 7-46. doi:10.1007/s00429-022-02512-y

Seghier, M. L., Fagan, E., & Price, C. J. (2010). Functional subdivisions in the left angular gyrus where the semantic system meets and diverges from the default network. *J Neurosci, 30*(50), 16809-16817. doi:10.1523/jneurosci.3377-10.2010

Seibert, T. M., Hagler, D. J., Jr., & Brewer, J. B. (2011). Early parietal response in episodic retrieval revealed with MEG. *Hum Brain Mapp, 32*(2), 171-181. doi:10.1002/hbm.21014

Sestieri, C., Shulman, G. L., & Corbetta, M. (2017). The contribution of the human posterior parietal cortex to episodic memory. *Nat Rev Neurosci, 18*(3), 183-192. doi:10.1038/nrn.2017.6

Siegel, M., Warden, M. R., & Miller, E. K. (2009). Phase-dependent neuronal coding of objects in short-term memory. *Proc Natl Acad Sci U S A, 106*(50), 21341-21346. doi:10.1073/pnas.0908193106

Simons, J. S., Ritchey, M., & Fernyhough, C. (2022). Brain Mechanisms Underlying the Subjective Experience of Remembering. *Annu Rev Psychol, 73*, 159-186. doi:10.1146/annurev-psych-030221-025439

Sirota, A., Montgomery, S., Fujisawa, S., Isomura, Y., Zugaro, M., & Buzsáki, G. (2008). Entrainment of neocortical neurons and gamma oscillations by the hippocampal theta rhythm. *Neuron, 60*(4), 683-697. doi:10.1016/j.neuron.2008.09.014

Solomon, E. A., Kragel, J. E., Sperling, M. R., Sharan, A., Worrell, G., Kucewicz, M., . . . Kahana, M. J. (2017). Widespread theta synchrony and high-frequency desynchronization underlies enhanced cognition. *Nature Communications, 8*(1), 1704. doi:10.1038/s41467-017-01763-2

Solomon, E. A., Stein, J. M., Das, S., Gorniak, R., Sperling, M. R., Worrell, G., . . . Kahana, M. J. (2019). Dynamic Theta Networks in the Human Medial Temporal Lobe Support Episodic Memory. *Curr Biol, 29*(7), 1100-1111.e1104. doi:10.1016/j.cub.2019.02.020

Spiers, H. J., Burgess, N., Maguire, E. A., Baxendale, S. A., Hartley, T., Thompson, P. J., & O'Keefe, J. (2001). Unilateral temporal lobectomy patients show lateralized topographical and episodic memory deficits in a virtual town. *Brain, 124*(Pt 12), 2476-2489. doi:10.1093/brain/124.12.2476

Spitzer, B., & Haegens, S. (2017). Beyond the Status Quo: A Role for Beta Oscillations in Endogenous Content (Re)Activation. *eNeuro, 4*(4). doi:10.1523/eneuro.0170-17.2017

Spreng, R. N., Stevens, W. D., Chamberlain, J. P., Gilmore, A. W., & Schacter, D. L. (2010). Default network activity, coupled with the frontoparietal control network, supports goal-directed cognition. *Neuroimage, 53*(1), 303-317. doi:10.1016/j.neuroimage.2010.06.016

Stangl, M., Topalovic, U., Inman, C. S., Hiller, S., Villaroman, D., Aghajan, Z. M., . . . Suthana, N. (2021). Boundary-anchored neural mechanisms of location-encoding for self and others. *Nature, 589*(7842), 420-425. doi:10.1038/s41586-020-03073-y

Stanley, D. A., Roy, J. E., Aoi, M. C., Kopell, N. J., & Miller, E. K. (2018). Low-Beta Oscillations Turn Up the Gain During Category Judgments. *Cereb Cortex, 28*(1), 116-130. doi:10.1093/cercor/bhw356

Summerfield, J. J., Hassabis, D., & Maguire, E. A. (2010). Differential engagement of brain regions within a 'core' network during scene construction. *Neuropsychologia, 48*(5), 1501-1509. doi:10.1016/j.neuropsychologia.2010.01.022

Tallon-Baudry, C., Bertrand, O., Hénaff, M. A., Isnard, J., & Fischer, C. (2005). Attention modulates gamma-band oscillations differently in the human lateral occipital cortex and fusiform gyrus. *Cereb Cortex, 15*(5), 654-662. doi:10.1093/cercor/bhh167

Tan, R. J., Rugg, M. D., & Lega, B. C. (2020). Direct brain recordings identify hippocampal and cortical networks that distinguish successful versus failed episodic memory retrieval. *Neuropsychologia, 147*, 107595. doi:10.1016/j.neuropsychologia.2020.107595

Trimper, J. B., Galloway, C. R., Jones, A. C., Mandi, K., & Manns, J. R. (2017). Gamma Oscillations in Rat Hippocampal Subregions Dentate Gyrus, CA3, CA1, and Subiculum Underlie Associative Memory Encoding. *Cell Rep, 21*(9), 2419-2432. doi:10.1016/j.celrep.2017.10.123

Trimper, J. B., Stefanescu, R. A., & Manns, J. R. (2014). Recognition memory and theta-gamma interactions in the hippocampus. *Hippocampus, 24*(3), 341-353. doi:10.1002/hipo.22228

Tulving, E. (2002). Episodic memory: from mind to brain. *Annu Rev Psychol, 53*, 1-25. doi:10.1146/annurev.psych.53.100901.135114

Uddin, L. Q., Supekar, K., Amin, H., Rykhlevskaia, E., Nguyen, D. A., Greicius, M. D., & Menon, V. (2010). Dissociable connectivity within human angular gyrus and intraparietal sulcus: evidence from functional and structural connectivity. *Cereb Cortex, 20*(11), 2636-2646. doi:10.1093/cercor/bhq011

Uncapher, M. R., & Wagner, A. D. (2009). Posterior parietal cortex and episodic encoding: insights from fMRI subsequent memory effects and dual-attention theory. *Neurobiol Learn Mem, 91*(2), 139-154. doi:10.1016/j.nlm.2008.10.011

Verhagen, J., & Wagenmakers, E. J. (2014). Bayesian tests to quantify the result of a replication attempt. *J Exp Psychol Gen, 143*(4), 1457-1475. doi:10.1037/a0036731

Vincent, J. L., Snyder, A. Z., Fox, M. D., Shannon, B. J., Andrews, J. R., Raichle, M. E., & Buckner, R. L. (2006). Coherent spontaneous activity identifies a hippocampal-parietal memory network. *J Neurophysiol, 96*(6), 3517-3531. doi:10.1152/jn.00048.2006

Vogt, B. A., & Pandya, D. N. (1987). Cingulate cortex of the rhesus monkey: II. Cortical afferents. *J Comp Neurol, 262*(2), 271-289. doi:10.1002/cne.902620208

Wagner, A. D., Paré-Blagoev, E. J., Clark, J., & Poldrack, R. A. (2001). Recovering meaning: left prefrontal cortex guides controlled semantic retrieval. *Neuron, 31*(2), 329-338. doi:10.1016/s0896-6273(01)00359-2

Wagner, A. D., Shannon, B. J., Kahn, I., & Buckner, R. L. (2005). Parietal lobe contributions to episodic memory retrieval. *Trends Cogn Sci, 9*(9), 445-453. doi:10.1016/j.tics.2005.07.001

Wang, J. X., Rogers, L. M., Gross, E. Z., Ryals, A. J., Dokucu, M. E., Brandstatt, K. L., . . . Voss, J. L. (2014). Targeted enhancement of cortical-hippocampal brain networks and associative memory. *Science, 345*(6200), 1054-1057. doi:10.1126/science.1252900

Wang, M. Y., Wang, J., Zhou, J., Guan, Y. G., Zhai, F., Liu, C. Q., . . . Luan, G. M. (2017). Identification of the epileptogenic zone of temporal lobe epilepsy from stereo-electroencephalography signals: A phase transfer entropy and graph theory approach. *Neuroimage Clin, 16*, 184-195. doi:10.1016/j.nicl.2017.07.022

Watrous, A. J., Tandon, N., Conner, C. R., Pieters, T., & Ekstrom, A. D. (2013). Frequency-specific network connectivity increases underlie accurate spatiotemporal memory retrieval. *Nature Neuroscience, 16*(3), 349-356. doi:10.1038/nn.3315

Wen, X., Liu, Y., Yao, L., & Ding, M. (2013). Top-down regulation of default mode activity in spatial visual attention. *J Neurosci, 33*(15), 6444-6453. doi:10.1523/jneurosci.4939-12.2013

Whitlock, J. R., Sutherland, R. J., Witter, M. P., Moser, M. B., & Moser, E. I. (2008). Navigating from hippocampus to parietal cortex. *Proc Natl Acad Sci U S A, 105*(39), 14755-14762. doi:10.1073/pnas.0804216105

Wilding, E. L., & Rugg, M. D. (1996). An event-related potential study of recognition memory with and without retrieval of source. *Brain, 119 (Pt 3)*, 889-905. doi:10.1093/brain/119.3.889

Wu, S. S., Chang, T. T., Majid, A., Caspers, S., Eickhoff, S. B., & Menon, V. (2009). Functional heterogeneity of inferior parietal cortex during mathematical cognition assessed with cytoarchitectonic probability maps. *Cereb Cortex, 19*(12), 2930-2945. doi:10.1093/cercor/bhp063

Zhang, S., & Li, C. S. (2012). Functional connectivity mapping of the human precuneus by resting state fMRI. *Neuroimage, 59*(4), 3548-3562. doi:10.1016/j.neuroimage.2011.11.023

Figure 1:

(a) Experiment 1 — VFR

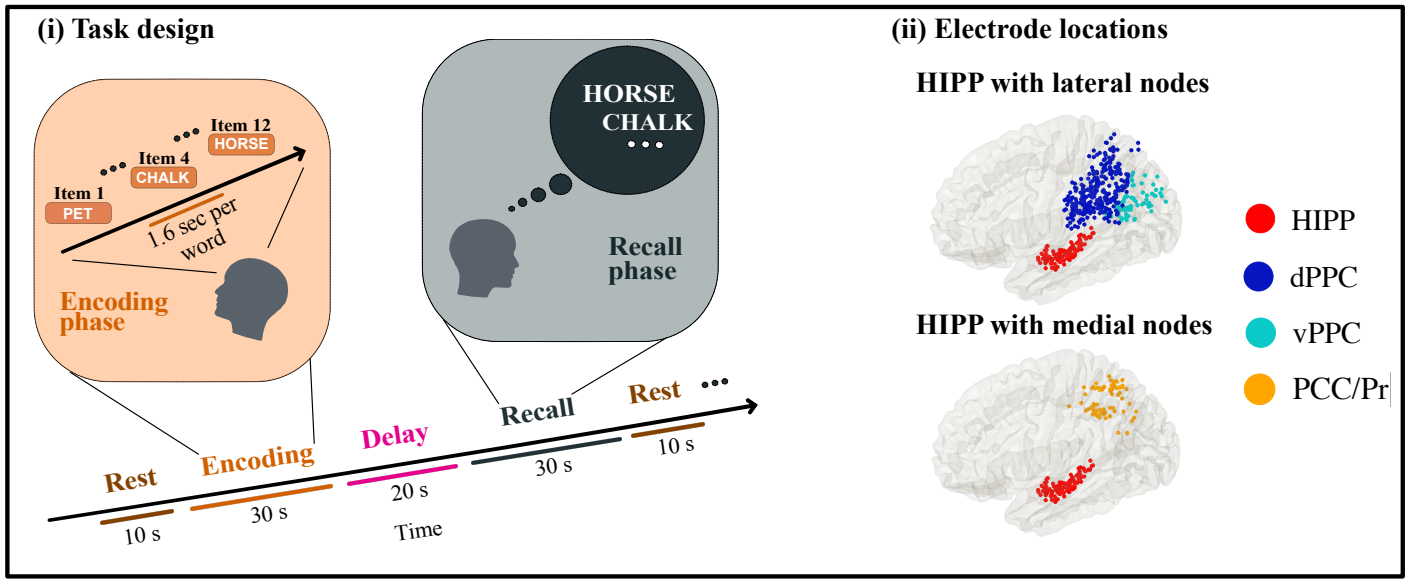

(b) Experiment 2 — CATVFR

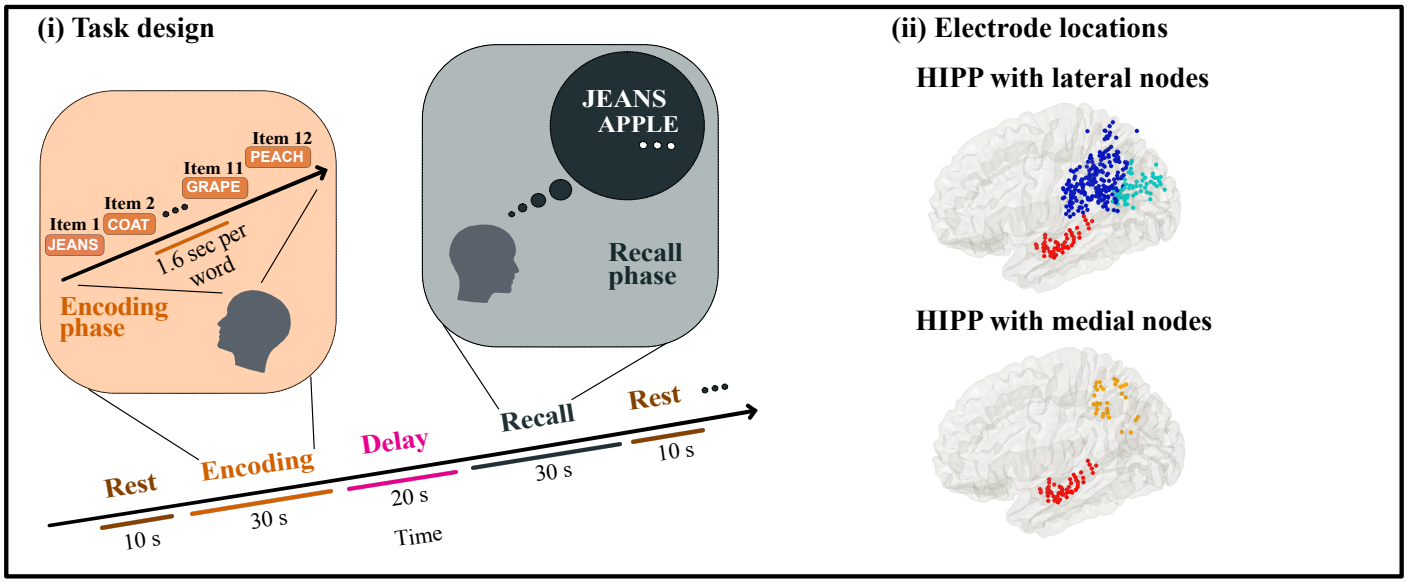

(c) Experiment 3 — WMSM

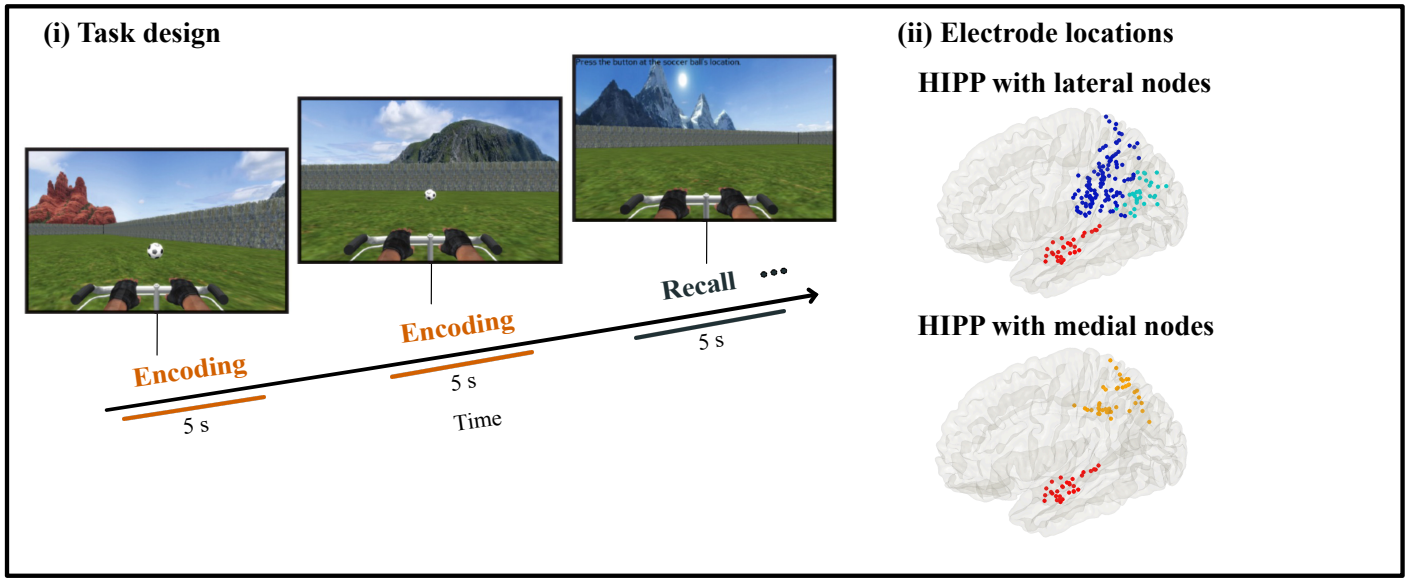

Figure 2:

(a) Experiment 1 — VFR

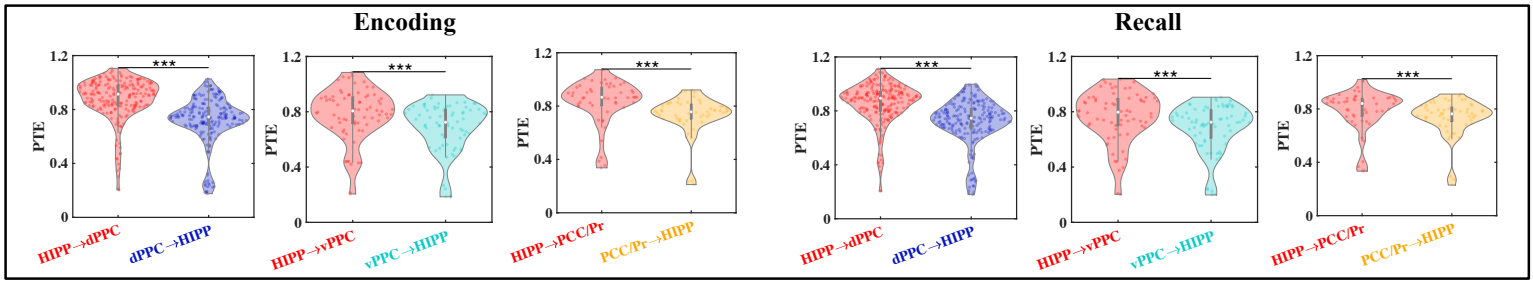

(b) Experiment 2 — CATVFR

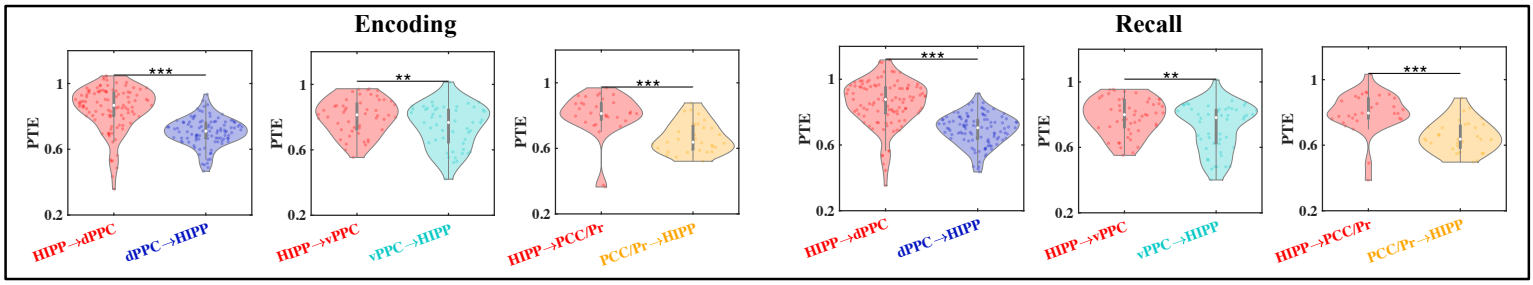

(c) Experiment 3 — WMSM

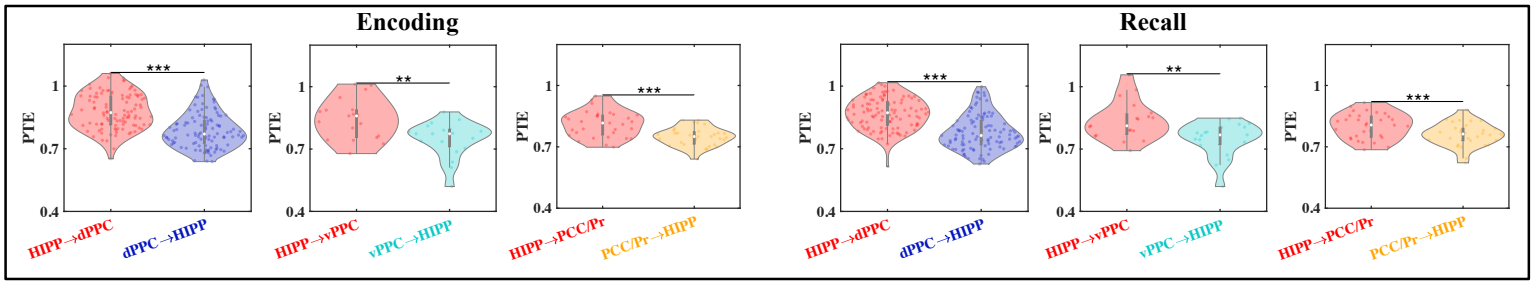

Figure 3:

(a) Experiment 1 — VFR

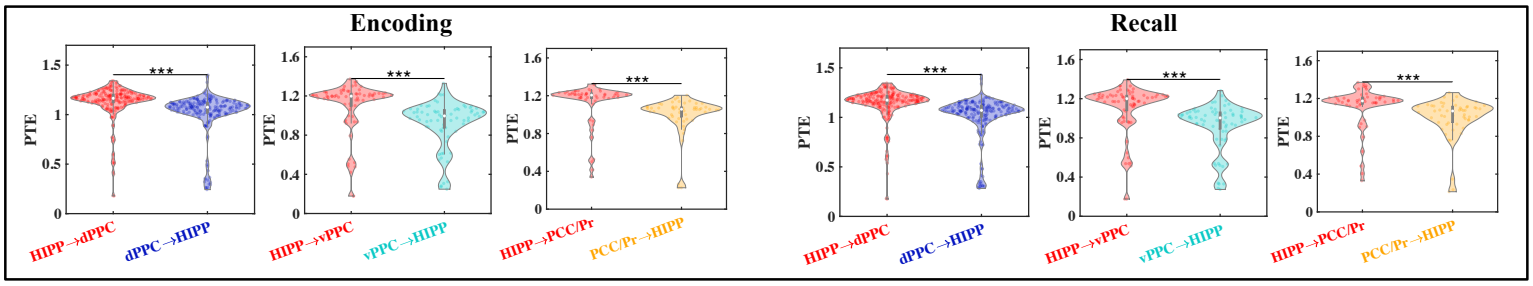

(b) Experiment 2 — CATVFR

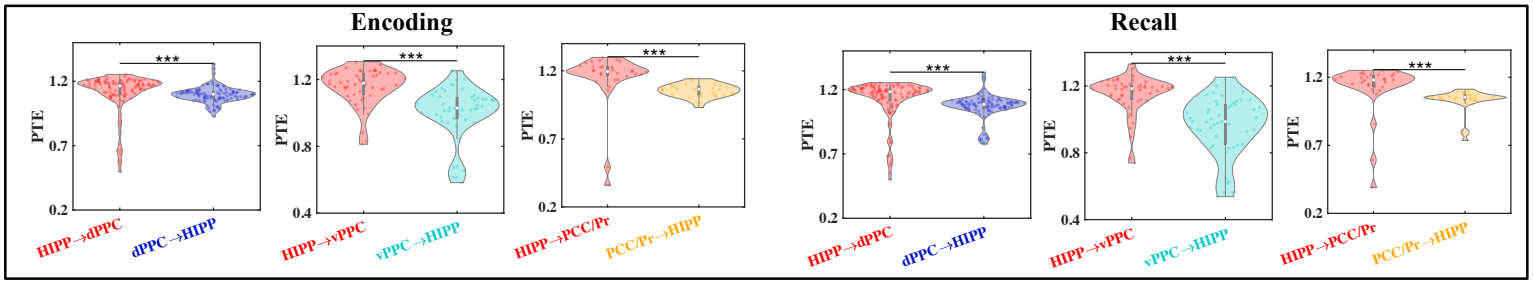

(c) Experiment 3 — WMSM

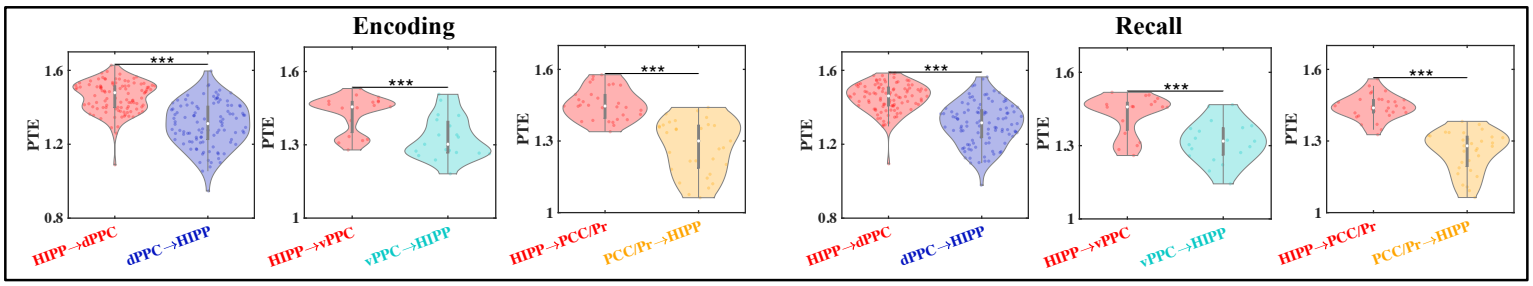

Figure 4:

(a) Experiment 1 — VFR

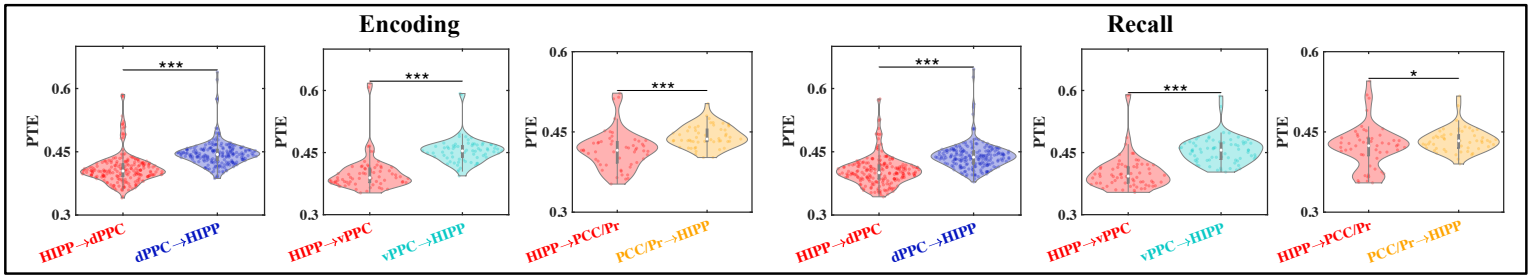

(b) Experiment 2 — CATVFR

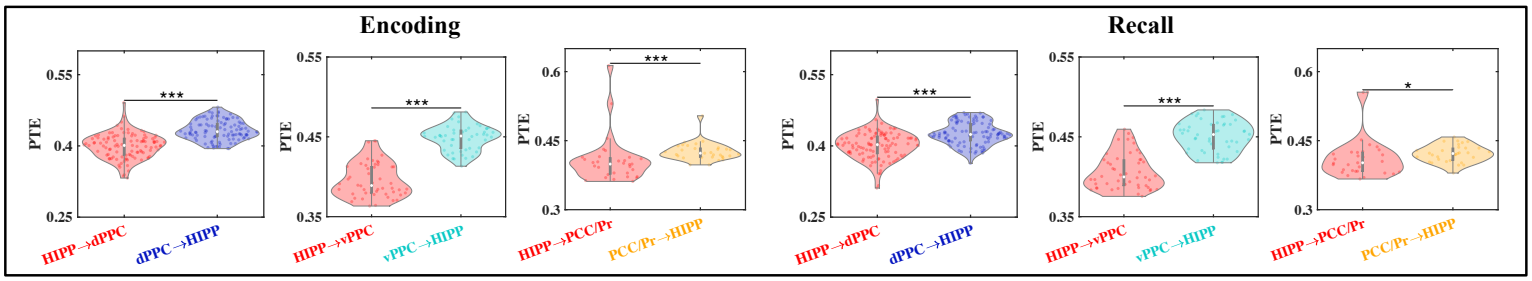

(c) Experiment 3 — WMSM

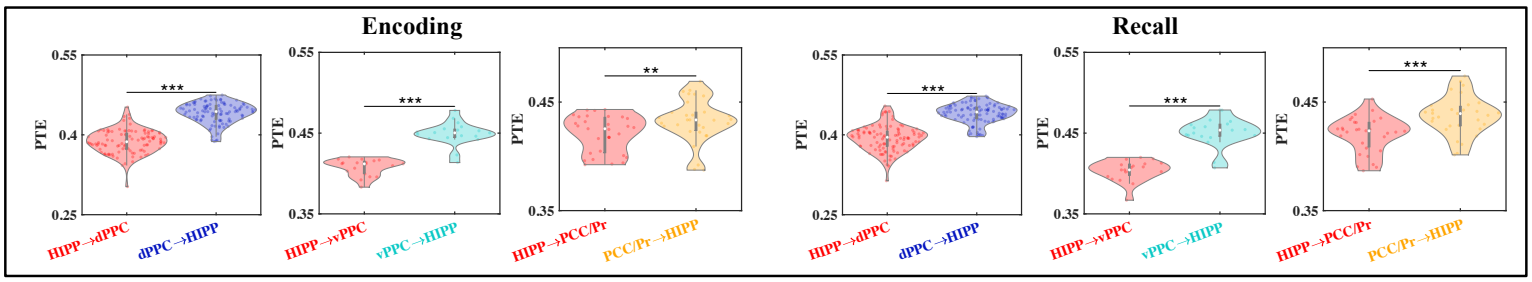

Figure 5:

(a) Experiment 1 — VFR

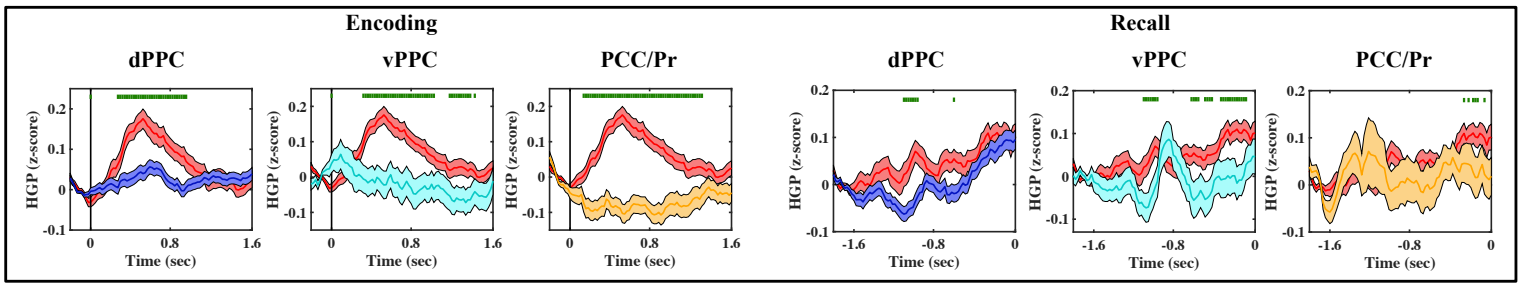

(b) Experiment 2 — CATVFR

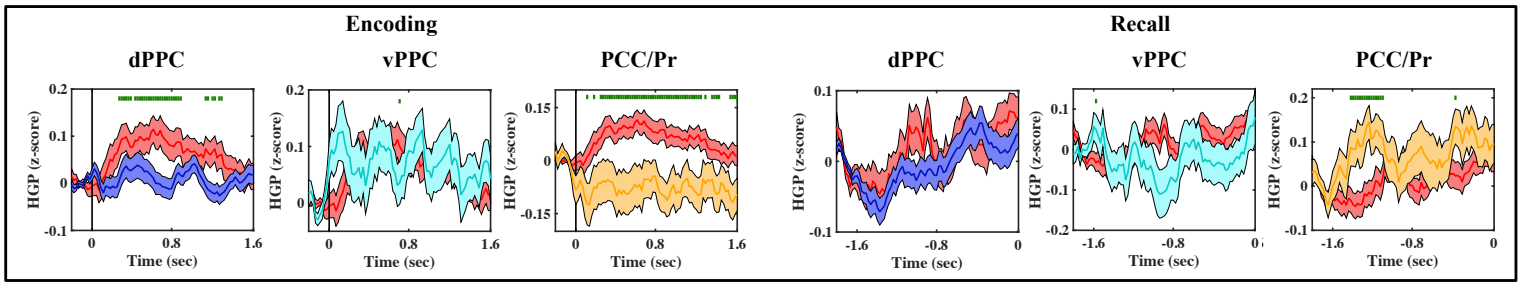

(c) Experiment 3 — WMSM

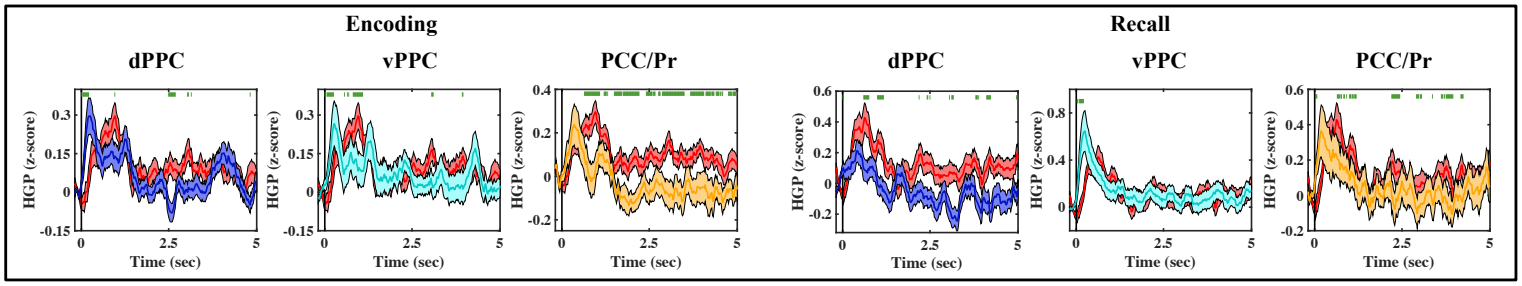

Figure 6:

(a) Broadband

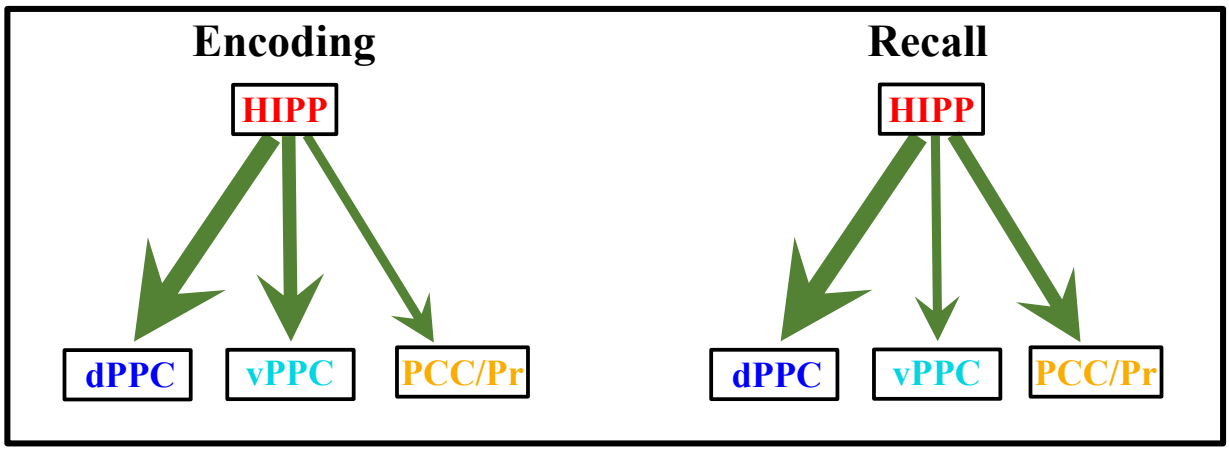

(b) Delta-theta

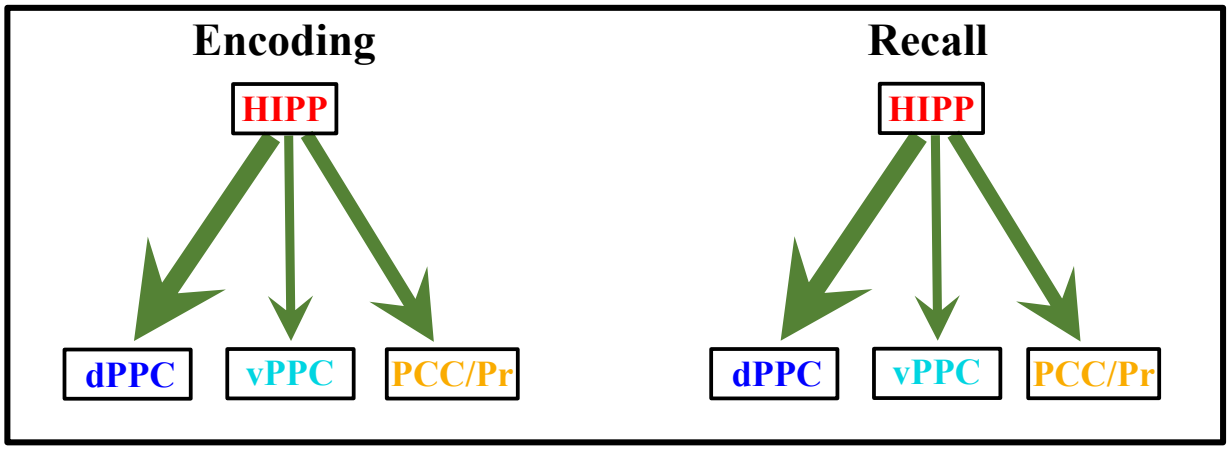

(c) Beta

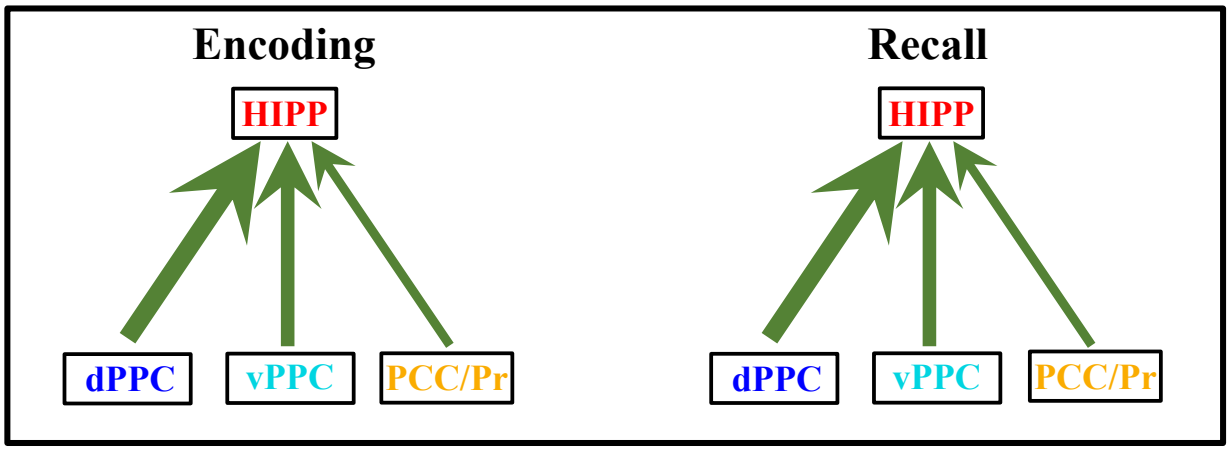

Supplementary Materials

I. Supplementary Figures (pages 2-3)

II. Supplementary Tables (pages 4-11)

Supplementary Figures

Figure S1. Directed information flow between hippocampus and dorsal and ventral subdivisions of the posterior parietal cortex (dPPC and vPPC) and PCC/precuneus (PCC/Pr) in gamma band (30-80 Hz). *** $p < 0.001$, ** $p < 0.01$, * $p < 0.05$ (Linear mixed effects ANOVA, FDR-corrected).

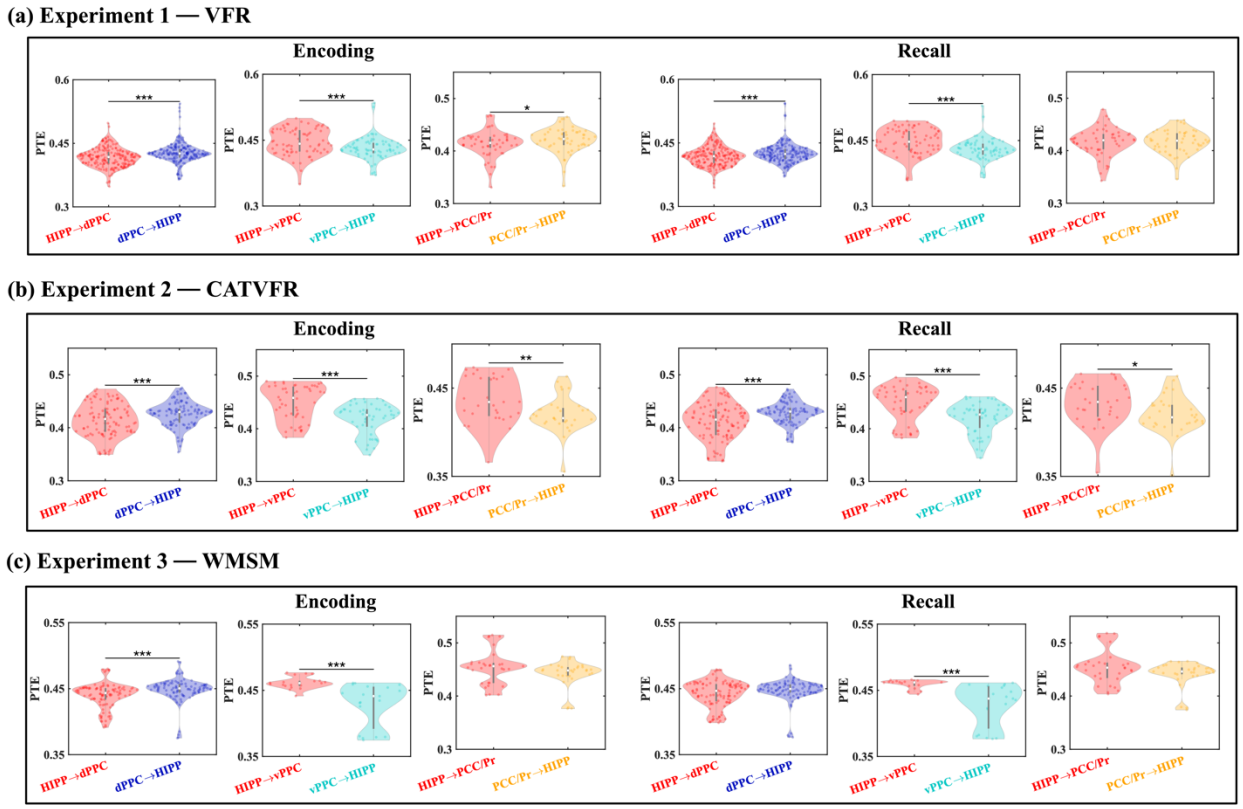

Figure S2. Directed information flow between hippocampus and dorsal and ventral subdivisions of the posterior parietal cortex (dPPC and vPPC) and PCC/precuneus (PCC/Pr) in high-gamma band (80-160 Hz). *** $p < 0.001$, ** $p < 0.01$, * $p < 0.05$ (Linear mixed effects ANOVA, FDR-corrected).

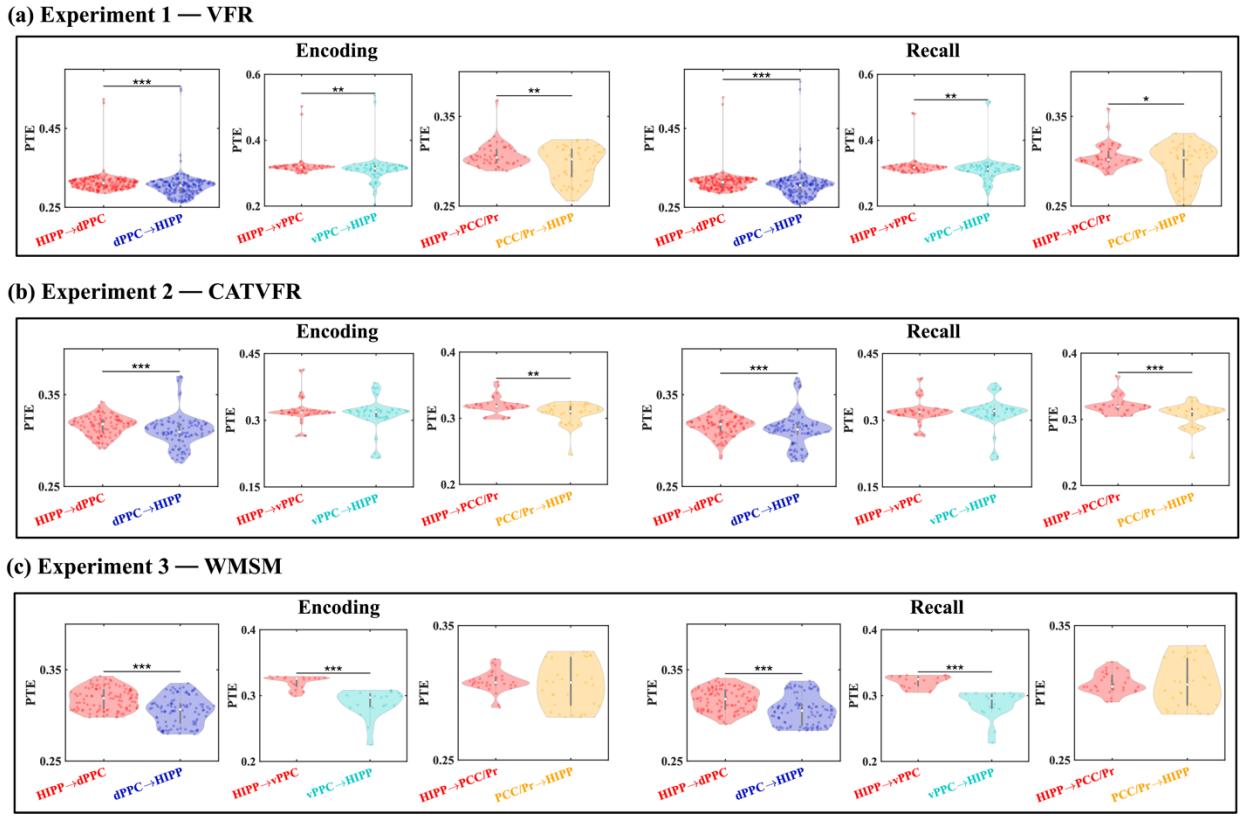

Supplementary Tables

Table S1. Participant demographic information (total 98 participants).

Participant ID	Gender	Age
002	F	49
003	F	39
006	F	20
008	F	55
010	F	30
014	F	47
015	F	54
018	M	47
021	M	34
024	F	36
030	M	23
032	F	19
033	F	31
034	F	29
035	F	45
036	M	49
044	M	58
049	F	52
050	M	20
051	F	24
052	F	19
054	M	23
059	F	44
063	M	23
065	F	34
066	M	39
067	F	45
069	M	26
070	F	40
073	M	60
074	M	24
075	M	50
076	M	29
080	F	43
081	F	33
083	F	49
084	M	25
089	M	36

092	M	44
094	M	47
101	F	26
102	M	34
108	F	23
111	M	20
114	F	31
119	F	26
120	F	33
122	F	48
124	F	40
125	F	44
130	M	57
134	M	64
135	M	47
137	F	21
138	M	41
144	M	53
147	M	47
151	M	36
153	M	38
154	F	36
158	F	45
161	F	53
163	M	45
164	M	37
168	M	24
173	F	18
174	M	29
175	M	34
177	F	23
180	F	21
187	F	51
190	F	57
193	M	37
195	M	44
196	M	18
203	F	36
204	F	25
207	F	39
221	M	57
223	F	42
227	M	32

228	F	58
230	F	56
232	M	27
234	M	25
236	F	51
239	M	27
240	F	37
245	M	30
247	F	61
260	F	57
279	F	57
286	F	57
292	F	39
297	M	24
298	F	24
299	M	43
302	M	48

Table S2a. Number of electrode pairs used in phase transfer entropy (PTE) analysis in the verbal free recall task. HIPP: hippocampus; dPPC: dorsal posterior parietal cortex; vPPC: ventral posterior parietal cortex; PCC: posterior cingulate cortex, Pr: precuneus.

Network pairs	Number of electrode pairs (n)	Number of participants	Participant IDs (Gender/Age)
HIPP-dPPC	208	23	003 (F/39), 010 (F/30), 035 (F/45), 049 (F/52), 054 (M/23), 065 (F/34), 066 (M/39), 080 (F/43), 111 (M/20), 114 (F/31), 120 (F/33), 134 (M/64), 135 (M/47), 138 (M/41), 151 (M/36), 161 (F/53), 164 (M/37), 174 (M/29), 195 (M/44), 236 (F/51), 240 (F/37), 297 (M/24), 299 (M/43)
HIPP-vPPC	72	13	010 (F/30), 032 (F/19), 033 (F/31), 111 (M/20), 120 (F/33), 134 (M/64), 154 (F/36), 161 (F/53), 174 (M/29), 195 (M/44), 203 (F/36), 230 (F/56), 240 (F/37)
HIPP-PCC/Pr	53	12	010 (F/30), 049 (F/52), 054 (M/23), 114 (F/31), 134 (M/64), 135 (M/47), 138 (M/41), 203 (F/36), 236 (F/51), 240 (F/37), 297 (M/24), 299 (M/43)

Table S2b. Number of electrode pairs used in phase transfer entropy (PTE) analysis in the categorized verbal free recall task. HIPP: hippocampus; dPPC: dorsal posterior parietal cortex; vPPC: ventral posterior parietal cortex; PCC: posterior cingulate cortex, Pr: precuneus.

Network pairs	Number of electrode pairs (n)	Number of participants	Participant IDs (Gender/Age)
HIPP-dPPC	105	12	035 (F/45), 065 (F/34), 066 (M/39), 092 (M/44), 111 (M/20), 114 (F/31), 119 (F/26), 135 (M/47), 144 (M/53), 174 (M/29), 240 (F/37), 245 (M/30)
HIPP-vPPC	50	7	021 (M/38), 032 (F/19), 111 (M/20), 119 (F/26), 174 (M/29), 230 (F/56), 240 (F/37)
HIPP-PCC/Pr	31	4	114 (F/31), 135 (M/47), 240 (F/37), 245 (M/30)

Table S2c. Number of electrode pairs used in phase transfer entropy (PTE) analysis in the water maze spatial memory task. HIPP: hippocampus; dPPC: dorsal posterior parietal cortex; vPPC: ventral posterior parietal cortex; PCC: posterior cingulate cortex, Pr: precuneus.

Network pairs	Number of electrode pairs (n)	Number of participants	Participant IDs (Gender/Age)
HIPP-dPPC	104	8	010 (F/30), 049 (F/52), 052 (F/19), 054 (M/23), 065 (F/34), 066 (M/39), 114 (F/31), 124 (F/40)
HIPP-vPPC	19	5	010 (F/30), 021 (M/34), 032 (F/19), 033 (F/31), 124 (F/40)
HIPP-PCC/Pr	31	5	010 (F/30), 049 (F/52), 054 (M/23), 114 (F/31), 124 (F/40)

Table S3a. Number of electrodes in each node used in high-gamma power analysis in the verbal free recall task. HIPP: hippocampus; dPPC: dorsal posterior parietal cortex; vPPC: ventral posterior parietal cortex; PCC: posterior cingulate cortex, Pr: precuneus.

Brain regions	Number of electrodes (n)	Number of participants	Participant IDs (Gender/Age)
HIPP	108	40	002 (F/49), 003 (F/39), 010 (F/30), 032 (F/19), 033 (F/31), 035 (F/45), 049 (F/52), 054 (M/23), 063 (M/23), 065 (F/34), 066 (M/39), 080 (F/43), 089 (M/36), 111 (M/20), 114 (F/31), 120 (F/33), 122 (F/48), 134 (M/64), 135 (M/47), 137 (F/21), 138 (M/41), 151 (M/36), 154 (F/36), 161 (F/53), 164 (M/37), 168 (M/24), 174 (M/29), 195 (M/44), 203 (F/36), 207 (F/39), 223 (F/42), 228 (F/58), 230 (F/56), 236 (F/51), 240 (F/37), 247 (F/61), 292 (F/39), 297 (M/24), 298 (F/24), 299 (M/43)
dPPC	297	54	003 (F/39), 010 (F/30), 015 (F/54), 018 (M/47), 030 (M/23), 035 (F/45), 036 (M/49), 044 (M/58), 049 (F/52), 050 (M/20), 054 (M/23), 059 (F/44), 065 (F/34), 066 (M/39), 067 (F/45), 069 (M/26), 070 (F/40), 074 (M/24), 075 (M/50), 080 (F/43), 084 (M/25), 094 (M/47), 101 (F/26), 102 (M/34),

			111 (M/20), 114 (F/31), 120 (F/33), 125 (F/44), 130 (M/57), 134 (M/64), 135 (M/47), 138 (M/41), 147 (M/47) , 151 (M/36), 153 (M/38), 158 (F/45), 161 (F/53), 163 (M/45), 164 (M/37), 173 (F/18), 174 (M/29), 177 (F/23), 193 (M/37), 195 (M/44), 196 (M/18), 204 (F/25), 232 (M/27), 234 (M/25), 236 (F/51), 240 (F/37), 260 (F/57), 286 (F/57), 297 (M/24), 299 (M/43)
vPPC	72	29	010 (F/30), 032 (F/19), 033 (F/31), 034 (F/29), 036 (M/49), 050 (M/20), 059 (F/44), 069 (M/26), 070 (F/40), 081 (F/33), 083 (F/49), 084 (M/25), 094 (M/47), 101 (F/26), 111 (M/20), 120 (F/33), 134 (M/64), 147 (M/47), 154 (F/36), 158 (F/45), 161 (F/53), 174 (M/29), 187 (F/51), 195 (M/44), 196 (M/18), 203 (F/36), 230 (F/56), 240 (F/37), 260 (F/57)
PCC/Pr	76	31	006 (F/20), 010 (F/30), 018 (M/47), 030 (M/23), 044 (M/58), 049 (F/52), 051 (F/24), 054 (M/23), 070 (F/40), 074 (M/24), 076 (M/29), 081 (F/33), 084 (M/25), 094 (M/47), 101 (F/26), 114 (F/31), 134 (M/64), 135 (M/47), 138 (M/41), 153 (M/38), 158 (F/45), 175 (M/34), 193 (M/37), 196 (M/18), 203 (F/36), 204 (F/25), 236 (F/51), 240 (F/37), 286 (F/57), 297 (M/24), 299 (M/43)

Table S3b. Number of electrodes in each node used in high-gamma power analysis in the categorized verbal free recall task. HIPP: hippocampus; dPPC: dorsal posterior parietal cortex; vPPC: ventral posterior parietal cortex; PCC: posterior cingulate cortex, Pr: precuneus.

Brain regions	**Number of electrodes (n)**	**Number of participants**	**Participant IDs (Gender/Age)**
HIPP	55	22	021 (M/38), 032 (F/19), 035 (F/45), 065 (F/34), 066 (M/39), 089 (M/36), 092 (M/44), 111 (M/20), 114 (F/31), 119 (F/26), 135 (M/47), 144 (M/53), 174 (M/29), 180 (F/21), 207 (F/39), 228 (F/58), 230 (F/56), 236 (F/51),

			239 (M/27), 240 (F/37), 245 (M/30), 247 (F/61)
dPPC	221	36	015 (F/54), 035 (F/45), 036 (M/49), 044 (M/58), 050 (M/20), 065 (F/34), 066 (M/39), 067 (F/45), 069 (M/26), 074 (M/24), 075 (M/50), 092 (M/44), 094 (M/47), 102 (M/34), 108 (F/23), 111 (M/20), 114 (F/31), 119 (F/26), 130 (M/57), 135 (M/47), 144 (M/53), 147 (M/47), 158 (F/45), 163 (M/45), 174 (M/29), 190 (F/57), 204 (F/25), 221 (M/57), 227 (M/32), 236 (F/51), 240 (F/37), 245 (M/30), 260 (F/57), 279 (F/57), 286 (F/57), 302 (M/48)
vPPC	63	19	021 (M/38), 032 (F/19), 036 (M/49), 050 (M/20), 069 (M/26), 083 (F/49), 094 (M/47), 111 (M/20), 119 (F/26), 147 (M/47), 158 (F/45), 174 (M/29), 187 (F/51), 190 (F/57), 221 (M/57), 230 (F/56), 240 (F/37), 260 (F/57), 302 (M/48)
PCC/Pr	33	12	044 (M/58), 074 (M/24), 094 (M/47), 114 (F/31), 135 (M/47), 158 (F/45), 204 (F/25), 227 (M/32), 236 (F/51), 240 (F/37), 245 (M/30), 286 (F/57)

Table S3c. Number of electrodes in each node used in high-gamma power analysis in the water maze spatial memory task. HIPP: hippocampus; dPPC: dorsal posterior parietal cortex; vPPC: ventral posterior parietal cortex; PCC: posterior cingulate cortex, Pr: precuneus.

Brain regions	**Number of electrodes (n)**	**Number of participants**	**Participant IDs (Gender/Age)**
HIPP	31	12	010 (F/30), 021 (M/34), 032 (F/19), 033 (F/31), 049 (F/52), 052 (F/19), 054 (M/23), 065 (F/34), 066 (M/39), 089 (M/36), 114 (F/31), 124 (F/40)
dPPC	117	21	010 (F/30), 014 (F/47), 015 (F/54), 018 (M/47), 024 (F/36), 030 (M/23), 044 (M/58), 049 (F/52), 050 (M/20), 052 (F/19), 054 (M/23), 065 (F/34), 066 (M/39), 067 (F/45), 069 (M/26), 074 (M/24), 075 (M/50), 101 (F/26), 114 (F/31), 124 (F/40), 177 (F/23)

vPPC	34	14	008 (F/55), 010 (F/30), 014 (F/47), 021 (M/34), 024 (F/36), 032 (F/19), 033 (F/31), 034 (F/29), 050 (M/20), 069 (M/26), 073 (M/60), 083 (F/49), 101 (F/26), 124 (F/40)
PCC/Pr	42	13	006 (F/20), 010 (F/30), 018 (M/47), 024 (F/36), 030 (M/23), 044 (M/58), 049 (F/52), 051 (F/24), 054 (M/23), 074 (M/24), 101 (F/26), 114 (F/31), 124 (F/40)